

**Chia (*Salvia hispanica*) gene expression atlas elucidates dynamic spatio-temporal changes associated with plant growth and development**

1 Parul Gupta<sup>1\*</sup>, Matthew Geniza<sup>1,2\*</sup>, Sushma Naithani<sup>1</sup>, Jeremy Phillips<sup>1</sup>, Ebaad Haq<sup>1</sup>, Pankaj

2 Jaiswal<sup>1#</sup>

3 \*Equal contribution and Co-First Authors

4

5 **Affiliations:**

6 <sup>1</sup>Department of Botany and Plant Pathology, Oregon State University, Corvallis, Oregon, USA

7 <sup>2</sup>Molecular and Cellular Biology Graduate Program, Oregon State University, Corvallis, Oregon,

8 USA

9

10 **# Correspondence:**

11 Pankaj Jaiswal

12 Department of Botany and Plant Pathology, Oregon State University, Corvallis, Oregon, USA

13 Phone: +1-541-737-8471

14 Fax: +1-541-737-3573

15 Email: [jaiswalp@science.oregonstate.edu](mailto:jaiswalp@science.oregonstate.edu)

16

17 **Running title:** Reference transcriptome atlas of Chia

18

19 **Abbreviations**

20 DAF: Days after flowering; DAS: Days after sowing.

21

22 **Abstract**

23 Chia (*Salvia hispanica* L.), now a popular superfood, is one of the richest sources of dietary  
24 nutrients such as protein, fiber, and polyunsaturated fatty acids. At present, the genomic and  
25 genetic information available in the public domain for this crop is scanty, which hinders  
26 understanding its growth and developmental processes and impedes genetic improvement  
27 through genomics-assisted methods. We report RNA-seq based comprehensive transcriptome  
28 atlas of Chia across 13 different tissue types covering vegetative and reproductive growth  
29 stages. We generated ~394 million raw reads from transcriptome sequencing, of which ~355  
30 million high-quality reads were used to generate *de novo* reference transcriptome assembly and  
31 the tissue-specific transcript assemblies. After quality assessment of merged assemblies and  
32 using redundancy reduction methods, 82,663 reference transcripts were identified. Of these,  
33 53,200 transcripts show differential expression in at least one sample and provide information on  
34 spatio-temporal modulation of gene expression in Chia. We identified genes involved in the  
35 biosynthesis of omega-3 and omega-6 polyunsaturated fatty acids, and various terpenoid  
36 compounds. The study also led to the identification of 633 differentially expressed transcription  
37 factors from 53 gene families. The coexpression analysis suggested that members of the B3,  
38 bZIP, ERF, WOX, AP2, MYB, C3H, EIL, LBD, DBB, Nin-like, and HSF transcription factor  
39 gene families play key roles in the regulation of target gene expression across various  
40 developmental stages. This study also identified 2,411 simple sequence repeat (SSRs) as  
41 potential genetic markers residing in the transcribed regions. The transcriptome atlas provides  
42 essential genomic resources for basic research, applications in plant breeding, and annotation of  
43 the Chia genome.

44

45 **Keywords:** Chia (*Salvia hispanica*), transcriptome (RNA-Seq), expression atlas, tissue-specific  
46 gene expression, omega-3 fatty acids, crop genetics

47

## 48 **Introduction**

49 *Salvia hispanica* L. (Chia), an annual herbaceous plant originally from Central America (Cahill,  
50 2005), is a member of the Lamiaceae (mint) family. Chia plants usually grow around one meter  
51 in height and produce raceme inflorescence bearing small purple flowers. Chia displays levels of  
52 cold and frost-tolerance, and its growth excels at higher altitudes (Ixtaina, Nolasco & Tomás,  
53 2008; Baginsky et al., 2016). It is cultivated primarily for its nutrient-rich seeds. Chia seeds are  
54 traditionally a core component of the Mayan and Aztec population's diet. Recently, its  
55 consumption has grown outside of South America due to its rich nutritional and gluten-free  
56 characteristics (Mohd Ali et al., 2012). The Chia seed contains approximately 40% oil by weight,  
57 of which the majority fraction is omega-3 and omega-6 polyunsaturated fatty acids (Mohd Ali et  
58 al., 2012). The seeds are gluten-free, rich in protein (15-20%), dietary fiber (20-40%), minerals  
59 (4-5%), and antioxidants (Reyes-Caudillo, Tecante & Valdivia-López, 2008; Ayerza (h) &  
60 Coates, 2009; Muñoz et al., 2013). These nutritional attributes have made Chia a desirable  
61 'superfood'. Several studies in humans and mouse models on a diet supplemented with Chia seed  
62 (Marcinek and Krejpcio, 2017; Oliva et al., 2013; Ullah et al., 2016; Valdivia-López and  
63 Tecante, 2015; Vuksan et al., 2017a, 2017b, 2010, 2007) report improvement in muscle lipid  
64 content, cardiovascular health, total cholesterol ratio, triglyceride content, and helped attenuate  
65 blood glucose levels in type-2 diabetes patients (Vuksan et al., 2007; Chicco et al., 2009; Peiretti  
66 & Gai, 2009; Oliva et al., 2013). Chia seeds come with variations of color and texture and may  
67 include black or dark spots. The Chia is known to show site of cultivation and environment-

68 dependent effects on the growth of the plant, seed protein and oil content, and fatty acid  
69 composition (Ayerza, 2009). No correlation was found between nutritional composition and seed  
70 color of Chia seeds, though it is positively correlated to geographic location and environmental  
71 differences where Chia plants are grown (Ayerza (h) & Coates, 2009; Ayerza, 2010). In addition  
72 to food, Chia is a rich source of other useful products. For example, plant leaves contain various  
73 essential oil components such as  $\beta$ -caryophyllene, globulol,  $\gamma$ -muroloeno,  $\beta$ -pinene,  $\alpha$ -humulene,  
74 germacrene, and widdrol that are known to have insect repellent or insecticidal properties  
75 (Amato et al., 2015; Elshafie et al., 2018).

76 High-throughput experiments have reported large amounts of genome-wide gene  
77 expression data from various oilseed crops such as *Glycine max*, *Arachis hypogaea*, *Camelina*  
78 *sativa* (Libault et al., 2010; Severin et al., 2010; Clevenger et al., 2016; Kagale et al., 2016).  
79 Whereas, only a handful of studies investigated fatty acid metabolism in Chia seeds (R. V. et al.,  
80 2015; Peláez et al., 2019) and to our knowledge none across different developmental stages of  
81 Chia. As we know, plant growth and development processes are controlled by the programmed  
82 expression of a wide array of genes at Spatial and temporal scales. Gene expression atlases help  
83 predict regulatory networks and gene clusters expressed in each tissue at different developmental  
84 stages which helped in revealing the key regulators of metabolic and developmental processes  
85 (Druka et al., 2006; Sekhon et al., 2011; Stelpflug et al., 2016; Cañas et al., 2017; Kudapa et al.,  
86 2018).

87 In spite of Chia being one of the traditionally valued plants in South America, there are  
88 limited genetics or genomics resources available to undertake functional and comparative  
89 genomics and design plant breeding projects. Therefore, we took an initiative to build genetic  
90 and genomic resources for this important crop for the community of plant researchers and



91 breeders. In this study, we describe tissue-specific gene expression atlas developed from 13  
92 tissues across the vegetative and reproductive stages of Chia (Table 1). Differential expression of  
93 transcripts involved in metabolic and regulatory pathways was examined. Furthermore, we added  
94 a functional-structural annotation to transcripts and identified potential simple sequence repeat  
95 (SSRs) molecular markers and pathway enrichment to learn about important metabolic pathways.  
96 The gene expression atlas presented here is a valuable functional genomics resource and a tool  
97 for accelerating gene discovery and breeding strategies in Chia.

98

## 99 **Results**

### 100 **Sequencing and de novo assembly**

101 The transcriptome of Chia was generated from 13 different tissue types, including mature dry  
102 seeds, seedling shoots, leaf stages, internode, inflorescence, and flowers (Table 1). The 101  
103 basepair (bp) length paired-end sequencing of the 39 cDNA libraries (prepared from the poly-A  
104 (mRNA) fraction of the total RNA from three biological replicates for each sample) resulted in  
105 393,645,776 sequence reads and approximately 80Gb of the nucleotide sequence (supplementary  
106 file S1). The high-quality reads were assembled for 65 and 75 k-mer lengths, and unique  
107 transcripts were generated after merging both k-mer assemblies for each tissue type. The  
108 number of assembled transcripts were observed in the range of 27,066 to 43,491 for tissue-  
109 specific assemblies (Fig. 1A). Among vegetative tissues, D69-P1-P2 showed maximum number  
110 (43,491), and seed showed the lowest number (27,066) of assembled transcripts (Fig. 1A).  
111 Among reproductive tissues, the maximum number of transcripts (43,418) with the highest  
112 average length of about 1000 bases was observed in the top half part of the D158-Raceme  
113 inflorescence (Fig. 1A). Total high-quality paired-end reads (352,976,255) from all tissue

114 libraries were pooled and assembled at 67 and 71 k-mer lengths using Velvet (Zerbino & Birney,  
115 2008) and Oases (Schulz et al., 2012). Chia transcript isoforms generated by each k-mer (67 and  
116 71 k-mer lengths) assembly were consolidated (referred to as merged assembly) to represent the  
117 total number of 145,503 unique transcripts of  $\geq 201$  bases in length (Fig. 1B).

118 As part of the quality assessment addressing redundancy, we first used the CD-HIT-EST  
119 algorithm (Li & Godzik, 2006) to reduce the number of redundantly assembled transcripts by  
120 grouped sequences displaying similarities higher than 90%. This yielded 82,663 transcripts (Fig.  
121 1B). This step was followed by running the transcriptome quality assessment software,  
122 TransRate (Smith-Unna et al., 2016). TransRate detects the redundant transcripts by aligning the  
123 reads to multiple transcripts, but the assignment process assigns them all to the transcript that  
124 best represents the canonical form. This process reduced the originally assembled transcriptome  
125 (145,503 transcripts) to 35,461 transcripts (Fig. 1B). We observed that the assembly produced by  
126 CD-HIT-EST experienced little to no loss in percentage of reads aligned. The assembly produced  
127 by TransRate, which utilizes Salmon (Patro et al., 2017) to estimate transcript abundance using  
128 map-based methods, contained nearly 50% less reads aligned in comparison to the CD-HIT-EST  
129 assembly. Furthermore, we used quality assessment tool QAST (Mikheenko et al., 2016) on the  
130 original assembly and each of the redundancy reduced assemblies (Supplementary file S2). The  
131 original and TransRate assemblies both had the better statistics in transcript number and length  
132 and both assemblies also contained the worst statistics in the complementing category  
133 (Supplementary file S2). The assembly produced by CD-HIT-EST represented the most  
134 moderate version of the assembly. Using the quality assessment and alignment data as criteria,  
135 we decided that the CD-HIT-EST assembly with 82,663 transcripts would be the most

136 appropriate for downstream analyses. Workflow for assembly and downstream analysis is  
137 showed in Supplementary file S3.

### 138 **Functional annotation of Chia transcriptome**

139 We compared the 82,663 assembled Chia transcripts to publically available genomes and gene  
140 models of Eudicots using BLASTx and tBLASTx (Mount, 2007) to estimate approximate  
141 coverage of genes represented in the assembled transcriptome (Fig. 1C). More than 84% of  
142 assembled Chia transcripts mapped to the closely related *Salvia miltiorrhiza* (Wenping et al.,  
143 2011) and *Salvia splendens* (Ge et al., 2014) transcriptomes (Fig. 1C). The dispersion of  
144 coverage within the genus is not surprising since the *Salvia* genus is very diverse. Both *S.*  
145 *miltiorrhiza* and *S. splendens* share a common center of origin in China, whereas *Salvia*  
146 *hispanica* originated in Central America. Within the Lamiaceae, about 56% of the transcripts  
147 mapped to members of the *Mentha* (mint) genus, namely, Watermint (*M. aquatica*), Peppermint  
148 (*M. piperita*), and Spearmint (*M. spicata*) (Ahkami et al., 2015a). Moving up the taxonomic rank  
149 to the order of Lamiales, 75% of Chia transcripts mapped to sesame (*Sesamum indicum*) (Zhang  
150 et al., 2013), an oilseed crop. A total of 71% and 74% of assembled Chia transcripts aligned to  
151 the model plant *Arabidopsis thaliana* and the *Solanum lycopersicum* (tomato) proteome set,  
152 respectively (Fig. 1C). Although assembled transcriptomes were not available, the RNA-Seq  
153 reads from two recently sequenced and publicly available *Salvia hispanica* projects (Sreedhar et  
154 al., 2015; Boachon et al., 2018) for seed (INSDC Accession PRJNA196477) and leaf tissues  
155 (INSDC Accession PRJNA359989) were aligned against our assembled chia transcriptome.  
156 About 69% sequence reads from the seed, and 43% of the leaf transcriptome sequences mapped  
157 to our assemblies.

158 Peptide sequences from the assembled transcripts were generated using TransDecoder,  
159 which scans all ORFs based on homology searches from Pfam and BlastP as ORF retention  
160 criteria. Out of total 82,663 transcripts, 65,587 transcripts from Chia were translated into 99,307  
161 peptides. The number of peptides is higher than the number of transcripts assembled due to  
162 multiple open reading frames (ORFs) occurring in a single transcript. Functional annotation of  
163 peptides was first carried out using InterProScan (Jones et al., 2014a) to assign structural-  
164 functional domains and then by employing agriGO (Du et al., 2010b). We were successful in  
165 assigning InterPro accessions to the 45,209 peptides (Supplementary file S4) and Gene Ontology  
166 (GO) terms to a total of 32,638 peptides (Supplementary file S5). A total of 20,857 peptides were  
167 with GO biological process (BP); 8,677 peptides were associated to GO cellular component  
168 (CC), and 26,877 peptides were annotated to GO molecular function (MF) terms (Supplementary  
169 file S5).

## 170 **Development of gene expression atlas**

171 A final set of 82,663 assembled transcripts and the RSEM (Li & Dewey, 2011b) package was  
172 used to estimate transcript abundance based on FPKM (Fragments Per Kilobase of transcript per  
173 Million mapped reads). After removing transcripts with extremely low/insignificant expression,  
174 we considered 82,385 transcripts for further analysis. In order to visualize cross-sample  
175 comparison, a heatmap of distance matrix was generated that showed hierarchical clustering of  
176 Pearson's correlations based upon FPKM values for all transcripts (Fig. 2). Most of the tissues  
177 clustered together based on developmental attributes that provide an intriguing clue about the  
178 spatial and temporal scale of the samples pattern. For example, vegetative tissues, D3 (cotyledon  
179 and shoot) and D12 (shoot and very first leaf at shoot apex), clustered together. Leaf stages  
180 varied at maturity level were also clustered together. Interestingly, we observed that seed and

181 internode tissues clustered together, suggesting that they share common transcripts. Similarly,  
182 among reproductive tissues, flowers (D159 and D164) and inflorescence tissues (raceme top and  
183 bottom half) clustered together.

184 In order to study the gene clusters with a similar expression, the expression trend of all  
185 transcripts across developmental stages were represented in 20 clusters (Supplementary file S6).  
186 Most of the transcripts in cluster #1 (7507 transcripts), #5 (4616 transcripts), #12 (3909  
187 transcripts), #15 (3619 transcripts), #18 (2679 transcripts), and #20 (2173 transcripts) showed  
188 higher expression in seeds, D3-tissues (cotyledon and shoot), mature leaf stage (D69-P5-6-7),  
189 flowers (D-159 and D-164), inflorescence (top half and bottom half) and internode, respectively  
190 (Supplementary file S6). Transcripts in cluster #1 enriched for LEA (Late embryogenesis  
191 abundant), seed storage proteins, oil body-associated proteins, and oleosin family members  
192 (Supplementary file S7). In soybean seed transcriptomes, storage protein genes like beta-  
193 conglycinins, oleosins, glycinins, several LEA proteins and dehydrin genes showed higher  
194 expression with respect to other genes (Severin et al., 2010; Jones & Vodkin, 2013). Cluster #5  
195 was considered rich in transcripts required for initial growth (D3-Cotyledon, D3-Shoot) of  
196 seedling after germination. The majority of highly expressed transcripts were annotated as zinc  
197 finger, basic leucine zipper family members, photosystem I and II related proteins, aquaporins,  
198 and calcineurin-like phosphoesterase domain-containing proteins (Supplementary file S7). In  
199 cluster #12, highly expressed transcripts in D69-P5-6-7 leaf stage were annotated as disease  
200 resistance proteins, leucine-rich receptor kinases (LRR-RLKs), and wall-associated receptor  
201 kinases (WAKs) (Supplementary file S7). Transcripts that encode transporter (ABC, phosphate,  
202 aluminum transporters) proteins, cytochrome P450s, glycosyltransferases, and WRKY  
203 transcription factors also enriched in this cluster. Cluster 15 represents transcripts that showed

204 higher expression in flowers. Transcripts annotated as beta-glucosidase, multidrug and toxic  
205 compound extrusion proteins, cinnamyl alcohol dehydrogenase (involved in lignin biosynthesis  
206 in floral stem in *Arabidopsis*) (Sibout et al., 2005), germin-like proteins (might play a role in  
207 plant defense), pectin acylesterases, MYB family transcription factors (MYB21 and MYB24),  
208 GDSL lipase family members, and cytochrome P450s were highly enriched in this cluster  
209 (Supplementary file S7). MYB21 and MYB24 transcription factors are known for their role in  
210 petal, stamen, and gynoecium development in flowers (Reeves et al., 2012). Cinnamyl alcohol  
211 dehydrogenases are involved in lignin biosynthesis in floral stem in *Arabidopsis* (Sibout et al.,  
212 2005), and germin-like proteins play an important role in response to pathogens (Zimmermann et  
213 al., 2006; Manosalva et al., 2009; Wang et al., 2013). Transcripts that are highly upregulated in  
214 inflorescence tissues grouped in cluster #18. Transcription factors that play a vital role in floral  
215 meristem development enriched in this cluster. For example - agamous-like MADS-box proteins  
216 and MYB family transcription factors (Supplementary file S7). MYBs and MADS-box  
217 transcription factors are essential regulators of various developmental processes (Zimmermann et  
218 al., 2004; Millar & Gubler, 2005; Yang et al., 2007; Gomez et al., 2011; Kobayashi et al., 2015).  
219 Cluster #20 enriched with the transcripts upregulated in the D69-Internode sample  
220 (Supplementary file S7). It includes expression of transcription factors from the MYB (MYB54,  
221 MYB52) and NAC domain-containing transcription factor families known for their role in the  
222 development of the vegetative internodes. MYB54, MYB52, and NAC transcription factors are  
223 also known to regulate secondary cell wall biosynthesis (Zhong et al., 2008; Grant et al., 2010;  
224 Cassan-Wang et al., 2013). Transcripts encode xyloglucan endotransglucosylase, which  
225 participates in cell wall construction of growing tissues, were also upregulated in internode  
226 (cluster 20) compared to other tissues. A set of transcripts encode for receptor-like protein

227 kinases, involved in the signaling pathways known to regulate cell expansion (Guo et al., 2009;  
228 Haruta et al., 2014) is upregulated in cluster 20.

### 229 **Differential expression at each growth stage**

230 A total of 53,200 unique transcripts were differentially expressed among all tissue types of which  
231 38,480 transcripts show  $\log_2$  fold change  $\geq 2$ . Seed shows the highest number of differentially  
232 expressed transcripts, followed by D69-P5-P6-P7, D69-Internode, and D12-P1 (Table 2). Only  
233 D3-cotyledon showed the higher number of transcripts were under the upregulated category  
234 compared to the downregulated ones, whereas in the other 12 tissues, this pattern was opposite  
235 (Table 2). Seed showed the maximum number of tissue-specific differentially expressed  
236 transcripts (13,450) followed by D69-P5-P6-P7, D69-internode, D12-P1, and D3-Cotyledon  
237 tissue types (Table 2). The maximum number of upregulated transcripts was observed in seed  
238 (6,284) followed by D3-Cotyledon (2,632), D69-P5-P6-P7 (1,884), D69-Internode (1,390), and  
239 D159-Flowers (1,274). Similarly, the maximum number of downregulated transcripts were also  
240 observed in seed (13,429), followed by D69-P5-P6-P7 (6,637), D69-Internode (5,163), D12-P1  
241 (3,976), and D164-Flowers (3,353).

242 Besides, the distribution of differentially expressed transcripts between different  
243 combinations of similar or related developmental stages was evaluated (Fig. 3). In the initial  
244 growth stages: seed, D3-cotyledon, D3-shoot, and D12-shoot tissues, only 213 differentially  
245 expressed transcripts were common, and 70%, 8.9%, 2.4%, and 2.5% transcripts were specific to  
246 seed, D3-Cotyledon, D3-shoot and D12-shoot tissues, respectively (Fig. 3A). The majority of  
247 transcripts highly upregulated ( $\log_2$  fold change  $\geq 10$ ) in seed but downregulated ( $\log_2$  fold  
248 change  $\leq -4$ ) in other initial growth stages are seed storage, and LEA proteins. Among all leaf  
249 developmental stages, only 1.6% of differentially expressed transcripts were common, and 5372,

250 1599, 1092, and 9938 transcripts were specific to D12-P1, D69-P1-P2, D69-P3-P4, and D69-P5-  
251 P6-P7, respectively (Fig. 3B). Transcripts encoding for LRR-RLKs, WAKs, and RHD3 domain-  
252 containing proteins were highly expressed in D69-P5-6-7 compared to other leaf developmental  
253 stages. In early leaf developmental stages (D12-P1 and D69-P1-P2), transcripts encoding for  
254 Growth Regulating Factors (GRF2, GRF5) and bHLH domain-containing (SPEECHLESS)  
255 transcription factors were highly expressed compared to those in the mature leaf stages. GRF  
256 transcription factors play an important role in leaf growth, and the bHLH SPEECHLESS factors  
257 are involved in stomata initiation and development (Kim et al., 2003; MacAlister et al., 2007;  
258 Kanaoka et al., 2008; Lampard et al., 2008). Among raceme inflorescence and flower tissues,  
259 only 2.8% (414) of differentially expressed transcripts were common, and 3315, 1689, 2591, and  
260 2648 transcripts were specific to RacemeTopHalf, RacemeBottomHalf, D159-Flowers, and  
261 D164-Flowers, respectively (Fig. 3C). The higher expression of transcripts that encode ZFP2 and  
262 MYB transcription factors, cinnamyl alcohol dehydrogenase, and pectin acylesterases showed up  
263 in flowers. ZFP2 controls floral organ abscission (Cai & Lashbrook, 2008), and cinnamyl alcohol  
264 dehydrogenases are involved in lignin biosynthesis in floral stem (Sibout et al., 2005).  
265 Transcripts annotated as terpene synthases show upregulation in flowers as compared to the  
266 inflorescence tissues. Transcripts annotated as oxidation-reduction related activities were highly  
267 enriched in flowers, inflorescence, D-69 leaf stages, and internode tissues, which indicated that  
268 ROS concentration increases during these growth stages as in other species (Rogers, 2012;  
269 Rogers & Munné-Bosch, 2016; Singh et al., 2016).

## 270 **Pathways enriched across different development stages**

271 The metabolic network representation across developmental stages of Chia were determined by  
272 mapping to KEGG (Kyoto Encyclopedia of Genes and Genomes) pathways. A total of 5,555



273 transcripts mapped to 464 pathways. The higher numbers of transcripts mapped to starch and  
274 sucrose metabolism (PATH:ko00500), fatty acid metabolism (PATH:ko01040), phenylpropanoid  
275 biosynthesis (PATH:ko00940), photosynthesis (PATH:ko00195), fatty acid biosynthesis  
276 (PATH:ko00061), and various amino acids metabolism processes (Supplementary file S8).  
277 The expression pattern of transcripts encoding the enzymes for fatty acid metabolism and  
278 unsaturated fatty acid (including omega-3 and omega-6) metabolism across different  
279 developmental stages was analyzed (Figure 4). Transcripts for acetyl-CoA carboxylase (EC  
280 6.4.1.2), the very first enzyme catalyzing the conversion of acetyl-CoA to malonyl-CoA in the  
281 fatty acid biosynthesis were highly expressed in all tissues except seeds. The malonyl group  
282 from malonyl-CoA is transferred to acyl carrier proteins (ACP) in the next step for further  
283 elongation. We identified transcripts for all the enzymes participating in the elongation steps.  
284 Acyl-ACP thioesterases (3.1.2.14) acts in the last steps of fatty acid biosynthesis and serves as a  
285 determining factor for the generation of a variety of fatty acids within an organism. Since, Chia  
286 seeds are very rich in unsaturated fatty acids: linoleic and  $\alpha$ -linolenic acids, genes involved in  
287 unsaturated fatty acids biosynthesis were queried for their expression pattern across all tissue  
288 types (Fig. 4B). Fatty acid desaturases (FADs) are the crucial enzymes to perform the  
289 desaturation of fatty acids. We identified 32 FAD transcripts from FAD2, FAD3, FAD6,  
290 FAD7 and FAD8 families (Table 3). Endoplasmic reticulum localized *FAD2* and plastid localized  
291 *FAD6* encode two  $\omega$ -6 desaturases required to convert oleic acid to linoleic acid ( $18:2^{\Delta 9,12}$ )  
292 (Zhang et al., 2012). The desaturation of linoleic acid ( $18:2^{\Delta 9,12}$ ) to  $\alpha$ -linolenic acid ( $18:3^{\Delta 9,12,15}$ )  
293 is catalyzed by the endoplasmic reticulum localized FAD3 and plastid localized FAD7 and  
294 FAD8 proteins (Dar et al., 2017; Xue et al., 2018).

295 Mint, a Lamiaceae family plant, is primarily known for the production of monoterpenes,  
296 e.g., menthol and limonene (Aharoni, Jongsma & Bouwmeester, 2005; Ahkami et al., 2015b);  
297 however, the majority of Chia terpenes are sesqui-, di-, and tri-terpenes (Ma et al., 2012; Triikka  
298 et al., 2015; Cui et al., 2015). In our Chia dataset, we observed the expression profile of  
299 transcripts involved in the biosynthesis of terpenoid backbone, monoterpenes, and sesqui-  
300 terpenes. Transcripts encoding enzymes for each catalytic step of terpenoid backbone  
301 synthesized by the MEP (2-C-methyl-D-erythritol 4-phosphate) and the mevalonate (MVA)  
302 pathways showed differential expression pattern among all tissue types (Fig. 5). Transcripts for  
303 monoterpene synthases such as 1,8-cineole synthase (EC 4.2.3.108), myrcene synthase (EC  
304 4.2.3.15), and linalool synthase (EC 4.2.3.25) were highly expressed in reproductive tissues (Fig.  
305 5), indicating that flowers are the prime site for the biosynthesis of essential oils known to have  
306 therapeutic properties. However, transcripts for the sesquiterpene synthases,  $\beta$ -caryophyllene  
307 synthase (EC 4.2.3.57),  $\alpha$ -humulene synthase (EC 4.2.3.104), Germacrene synthase (EC  
308 4.2.3.60), and solavetivone oxygenase (EC 4.2.3.21), known for plant herbivory defense  
309 enriched in the vegetative tissues (Fig. 5).

### 310 **Transcription factor network**

311 Transcription factors are the key regulators that control many biological processes in plants,  
312 including growth and development. To gain detailed information about transcription factors, we  
313 investigated Chia transcriptome and identified 633 differentially expressed transcripts annotated  
314 to 53 transcription factor families (Supplementary file S9). The highest number of transcripts  
315 belong to MYB (60), followed by bHLH (45), NAC (38), bZIP (32), WRKY (28), C2H2 (27),  
316 MYB-related (25), MADS-box (26), C3H (24), G2-like (22), Hd-ZIP (22), Trihelix (17), TCP  
317 (14), Dof (13), GATA (13), GRAS (13), and TALE (13) gene families, etc.. The expression

318 pattern of differentially expressed transcription factors across developmental stages is shown in  
319 Fig. 6A.

320 To gain insight into the regulatory role of transcription factors in Chia, we filtered out  
321 highly upregulated transcription factors in any of the 13 tissues ( $\geq 5 \log_2$  fold change) to build a  
322 coexpression network. In an in-silico experiment, we used 23 transcription factors as baits  
323 (nodes) and FPKM values of 38,480 transcripts as an expression matrix. This analysis revealed a  
324 total of 1,98,746 connections (edges) among 23 bait transcript nodes and 11,055 differentially  
325 expressed transcript nodes (Fig. 6B). Two transcription factors, Sh\_Salba\_v2\_130985,  
326 Sh\_Salba\_v2\_121906 highly expressed in D69-Internode but downregulated or absent in other  
327 tissues, were annotated as MYB and C3H family members, respectively. Both the transcription  
328 factors connected to a set of 1,593 transcripts that showed no connection to any other bait nodes.  
329 A set of 16 transcripts solely connected to sh\_salba\_v2\_112851 an ERF transcription factor that  
330 was highly upregulated ( $\log_2$  fold change 5.561) in seed. All correlated 15 transcripts were  
331 downregulated in seed and other tissue types. The MYB transcription factor transcript  
332 sh\_salba\_v2\_131530 was upregulated in seed and connected to a set of 59 transcripts that were  
333 downregulated in seed and other tissues. Two transcripts (sh\_salba\_v2\_32610,  
334 sh\_salba\_v2\_03332), that downregulated in seed showed a connection to B3-domain containing  
335 sh\_salba\_v2\_89434 bait. A transcript (sh\_salba\_v2\_86132), downregulated in seed and  
336 annotated as disease resistance protein correlated to a HSF transcription factor bait transcript  
337 sh\_salba\_v2\_80249. A set of 14 transcripts downregulated in seed and D69-Internode were  
338 connected to all 23 bait transcripts. Bait transcripts also correlated to each other suggesting a  
339 multiple regulatory modules within the network (Fig. 6B).

340 **Identification of Simple Sequence Repeat molecular markers**

341 Simple Sequence Repeats (SSRs) are an important class of genetic markers widely used in  
342 molecular breeding applications. SSRs identified from the transcriptome are highly  
343 advantageous as compared to SSRs identified from the genome. If the SSRs identified from the  
344 transcribed region is polymorphic, they may have a direct impact on the expression, structure,  
345 stability of the open reading frame, and altered peptide sequence and functional domains. We  
346 identified a total of 2,411 SSRs in the *de novo* assembled transcriptome represented by di-, tri-,  
347 and tetra-nucleotide motifs (Supplementary file S10). The most abundant di-, tri, and tetra-  
348 nucleotide motifs were CT (201), GAA (84), and AGTC (12), respectively (Supplementary file  
349 S11). A total of 1,771 SSRs were present in the significantly differentially expressed transcripts,  
350 and 148 SSR markers found in the expressed transcripts mapped to at least one metabolic  
351 pathway (Supplementary file S12).

352

### 353 **Discussion**

354 At present, the genetic information and genomic resources on Chia are scanty. Before this work,  
355 a couple of studies focused on the expression of lipid biosynthesis genes in developing Chia  
356 seeds has been reported (Sreedhar et al., 2015; Peláez et al., 2019; Wimberley et al., 2020). Big  
357 data biology can fill in this gap and build reference resources for breeding and improvement of  
358 this important crop. Using RNA-Seq coupled with the *de-novo* transcriptome assembly approach,  
359 we developed a comprehensive gene-expression atlas for Chia from 13 different tissue samples  
360 (see Table 1) collected at various developmental stages of plants. Assembled transcripts were  
361 annotated using BLASTx and tBLASTx and then translated into peptides using Transdecoder  
362 (v2.1.0) with a minimum peptide length of 50 or more amino acids. The derived peptide set was  
363 subjected to InterProScan (Zdobnov & Apweiler, 2001a) and AgriGO (Du et al., 2010a) analyses

364 to assign structurally conserved domains and GO terms. Overall, the Chia transcriptome dataset  
365 is diverse, representing a majority of peptides belong to the cellular metabolic process, catalytic  
366 activity, regulation of gene expression, transport, ion binding, organelle, nucleus and  
367 macromolecular complexes. A comparison of Chia transcripts data sets to genomic/transcriptome  
368 datasets (Figure 1C) from the six most closely related eudicots including topmost matching with  
369 transcripts of perennial herbs, the red sage *Salvia miltiorrhiza* (Wenping et al., 2011) and the  
370 scarlet sage, *Salvia splendens* (Ge et al., 2014) - both species-rich in secondary metabolites  
371 known for their use in traditional medicine. In *de novo* assembled transcripts, the read mapping  
372 ambiguity is prevalent, and other popular tools, such as edgeR (Robinson, McCarthy & Smyth,  
373 2010) and DESeq (Anders & Huber, 2010) do not take variance due to read mapping uncertainty  
374 into consideration. Therefore, we employed EBSeq (Leng et al., 2013) for conducting differential  
375 gene expression analysis that takes variance due to the sequence read mapping ambiguity into  
376 account by grouping the isoforms.

377 This comprehensive expression atlas facilitated in the mining of gene expression data for  
378 regulatory and metabolic processes, tissue-specific gene expression pattern, and provided  
379 insights about functional relatedness of genes and their expression across developmental stages.  
380 Hierarchical clustering of Chia transcripts suggested the role of different gene families in the  
381 development of each growth stage, thus providing a foundation for studying the molecular  
382 mechanisms occurring in different tissues and developmental stages. For example, seed-specific  
383 transcripts: seeds are rich in storage, and LEA proteins are required for seed germination and  
384 embryogenesis. The Leaf-specific transcripts: mature leaves have higher expression of LRR-  
385 RLKs and WAKs proteins. LRR-RLKs are involved in guard cells and stomatal patterning  
386 (Shpak et al., 2005), and resistance to pathogens. GRF family transcription factors play an

387 essential role in the growth and development of leaf, were highly expressed in D69-P1-P2 leaf  
388 stages. In Arabidopsis, GRF1, GRF2, and GRF5 regulate leaf number and size (Kim, Choi &  
389 Kende, 2003; Horiguchi, Kim & Tsukaya, 2005; Lee et al., 2009).

390 The flower-specific transcripts show higher expression of terpene synthases, which  
391 suggested that as a characteristics of Lamiaceae family, Chia flowers are also rich in  
392 monoterpene synthases, e.g., 1, 8-cineole synthase (EC 4.2.3.108) and  $\beta$ -myrcene synthase (EC  
393 4.2.3.15). Cineole and myrcene are found in fragrant plants and are known to have therapeutic  
394 properties such as sedative, anti-inflammatory, antispasmodic, and antioxidant (do Vale et al.,  
395 2002; Moss & Oliver, 2012; Bouajaj et al., 2013; Juergens, 2014; Khedher et al., 2017). The  
396 reproductive versus vegetative tissue comparison shows that monoterpene synthases were  
397 expressed highly in reproductive tissues, and sesquiterpene synthases were prominent in  
398 vegetative tissues. These findings confirm that flowers are involved in the synthesis of fragrance  
399 and therapeutic essential oils, whereas vegetative tissues are rich in herbivory defense and  
400 insecticidal compounds.

401 Chia seeds are a rich source of polyunsaturated fatty acids. We observed lower  
402 expression of FAD transcripts in seeds as compared to other tissue types. This suggested that  
403 seed might serve as a storage organ for polyunsaturated fatty acids rather synthesis site or seeds  
404 we used in this study were dry and in semi-dormant condition. Essential oils, the secondary  
405 metabolic plant products of the terpenoid pathway produced by Lamiaceae plant family  
406 members, are highly desired for their usage in medicine, food, cosmetics, and for their  
407 agronomic properties such as insecticides, herbivory, and pathogen defense. In this Chia dataset,  
408 we identified transcripts encoding enzymes for terpenoid backbone (MVA and MEP) pathways.  
409 Monoterpene synthases are involved in essential oil biosynthesis, and sesquiterpene synthases

410 are primarily involved in the biosynthesis of insecticidal compounds. Phenylpropanoid and  
411 flavonoid biosynthesis pathways are also highly enriched in seeds and other tissue types  
412 (Supplementary file S8). These pathways synthesize precursors for various secondary  
413 metabolites and antioxidants vital for human health and thus make seeds more nutritious.

414 The correlation analysis gave us a hint of a significant relationship between highly  
415 upregulated transcription factors, and the other differentially expressed transcripts. We observed  
416 that MYB and C3H zinc finger transcription factors were highly upregulated in D69-Internode.  
417 Recent studies revealed that both transcription factor types are involved in internode elongation  
418 and development processes (Zhong et al., 2008; Kebrom, McKinley & Mullet, 2017; Gómez-  
419 Ariza et al., 2019). Sh\_Salba\_v2\_112851, an AP2/ERF family member, is highly expressed in  
420 seed only and might play a role in dehydration-induced response as DREB2A proteins that are  
421 involved in response to drought, salt, and low-temperature stress (Nakashima et al., 2000;  
422 Sakuma et al., 2002). A set of 15 transcripts, correlated with Sh\_Salba\_v2\_112851, were  
423 downregulated in seed, and participate in pathways that are downregulated in seed. For example-  
424 sh\_salba\_v2\_33433 (CONSTANS-like 10) might be involved in the regulation of flowering  
425 genes (Tan et al., 2016), sh\_salba\_v2\_01428 (histidine kinase 4) in cytokinin signaling (Ueguchi  
426 et al., 2001; Nishimura et al., 2004), sh\_salba\_v2\_107585 (microtubule regulatory protein) in  
427 hypocotyl cell elongation (Liu et al., 2013), and sh\_salba\_v2\_52914 (Apyrase) in normal growth  
428 and development of plant (Wolf et al., 2007). The correlation analysis suggests that transcription  
429 factors upregulated in seed and D69-internode tissues regulate various biological processes by  
430 controlling the expression of their target transcripts.

431 Further analysis of *de novo* assembled Chia transcriptome revealed 2,411 SSRs (see  
432 Supplementary file S11). Simple Sequence Repeats (SSRs) are an important class of genetic

433 markers widely used in molecular breeding applications. SSRs identified in chia reference  
434 transcriptome might be a valuable resource for breeding and genetic improvement of the crop.  
435 Overall, this is the first study that generated a tissue-specific reference transcriptome atlas for a  
436 Chia, a neo model and an agronomically important crop.

437

## 438 **Materials and Methods**

### 439 **Plant material, growth conditions and sampling**

440 Seeds of Chia (*Salvia hispanica* L.) bought online from Ancient Naturals, LLC, Salba Corp,  
441 N.A. were sown in autoclaved soils and watered thoroughly under controlled greenhouse  
442 conditions. All seeds germinated on the third day after sowing. Since the primary seed material  
443 was expected to a heterogeneous mixture, biological replicates for each tissue type were  
444 collected from three randomly chosen plants. The description of the samples collected from  
445 various developmental stages and tissue types is shown in Table 1. The tissue samples include  
446 seeds, cotyledons, shoots from 3 and 12 days old seedlings, leaves from 12 (D12-P1) and 69  
447 days old plants (D69-P1-P7), internode from 69 days old plants, raceme inflorescence from 158  
448 days old plants, and flowers from 1 and 5 days post-anthesis. Collected samples were  
449 immediately frozen in liquid nitrogen and stored at -80°C.

### 450 **Sample preparation and sequencing**

451 Total RNA from frozen tissues was extracted as per manufacturer's protocol using RNA Plant  
452 reagent (Invitrogen Inc., USA), RNeasy kits (Qiagen Inc., USA), and treated with RNase-free  
453 DNase (Life Technologies Inc., USA). Total RNA concentration and quality were determined  
454 using ND-1000 spectrophotometer (Thermo Fisher Scientific Inc., USA) and Bioanalyzer 2100  
455 (Agilent Technologies Inc., USA). Samples were prepared separately from each of the three



456 biological replicates of each tissue type using the TruSeq™ RNA Sample Preparation Kits (v2)  
457 and sequenced using the Illumina HiSeq 2500 instrument (Illumina Inc., USA) at the Center for  
458 Genomic Research and Biocomputing, Oregon State University.

#### 459 **De novo transcriptome assembly and quality estimation**

460 FASTQ file generation from the RNA-Seq sequences was done by CASAVA software v1.8.2  
461 (Illumina Inc.). Read quality was assessed using FastQC, and poor-quality reads were removed  
462 with Sickle v. 1.33 (-q = 20) (“najoshi/sickle”). The transcripts were assembled using Velvet  
463 (v1.2.10), which uses De Bruijn graphs to assemble short reads (Zerbino & Birney, 2008). An  
464 assembly of 67 and 71 k-mer lengths was performed using all tissue-specific reads. Assemblies  
465 produced by Velvet were merged into a single consensus assembly by Oases (v0.2.08) (Schulz et  
466 al., 2012), which produced transcript isoforms using read sequence and pairing information.  
467 Quality estimation to reduce redundancy in transcript assembly (a quality control check for *de*  
468 *novo* assembled transcriptome) was carried out using CD-HIT-EST (Li & Godzik, 2006),  
469 TransRate (Smith-Unna et al., 2016), and QUILT (Gurevich et al., 2013) software packages.  
470 The assembled transcripts passing the CD-HIT-EST quality control step were used for further  
471 downstream analyses and considered as a reference transcriptome for differential gene  
472 expression analyses.

#### 473 **Functional annotation and pathway enrichment analysis**

474 Assembled transcripts were annotated using BLASTx and tBLASTx with an E-value cutoff of  
475  $10^{-10}$ . The assembled transcripts were translated into peptides using Transdecoder (v2.1.0)  
476 (“TransDecoder (Find Coding Regions Within Transcripts)”) with a minimum peptide length of  
477 50 or more amino acids. Transdecoder used the BLASTp and PfamA search results to predict the  
478 translated ORF. Resulting peptides were analyzed using InterProScan Sequence Search

479 (v5.17.56) (Zdobnov & Apweiler, 2001b; Jones et al., 2014b) hosted by the Discovery  
480 Environment and powered by CyVerse (Joyce et al., 2017). We used the AgriGO Analysis  
481 Toolkit (Du et al., 2010b) to identify statistically enriched function groups of transcripts. AgriGO  
482 uses a Fisher's exact test with a Yekutieli correction for false discovery rate calculation.  
483 Significance cutoffs were set at a P-value of 0.05 and a minimum of 5 mapping entries per GO  
484 term. KAAS-KEGG automation server was used for orthologue assignment and pathway  
485 analysis (Moriya et al., 2007).

#### 486 **Gene expression and clustering**

487 Bowtie2 (Langmead & Salzberg, 2012) was used to align sequence reads from each tissue type  
488 to the assembled transcriptome. The RSEM software package (Li & Dewey, 2011a) was used to  
489 estimate the transcript expression counts (FPKM) from the aligned sequence reads. Count data  
490 obtained from RSEM was used in EBSeq (Leng et al., 2013) to identify differentially expressed  
491 genes based on the False Discovery Rate Corrected P-value of 0.05. Heatmaps were generated  
492 using Morpheus (Gould) developed by Broad Institute  
493 (<https://software.broadinstitute.org/morpheus>) and MEV (version 4.8.1) (*mev*, 2017) was used to  
494 cluster expression data from Chia. Log<sub>2</sub> transformed fold change value for each transcript was  
495 used as input (p-value 0.1). Due to the orders of magnitude in the expression of transcripts  
496 between tissue types, we chose several methods of data normalization for cluster generation.  
497 Unit variance, median centering of transcripts, and summation of squares were applied to the  
498 dataset. In the investigation of individual gene families, transcripts were hierarchically clustered  
499 using a Pearson correlation.

#### 500 **Coexpression and network analysis**

501 The transcription factor transcripts were classified based on homology searches in Plant TFDB  
502 database v5.0 (<http://planttfdb.cbi.pku.edu.cn>) (Jin et al., 2017) and BlastX searches against  
503 *Arabidopsis thaliana*. For the coexpression analysis, CoExpNetViz tool (Tzfadia et al., 2015)  
504 was used. This tool utilizes a set of query or bait genes as an input and a gene expression dataset.  
505 Transcription factor transcripts displaying maximum expression cutoff of  $\log_2$  transformed  
506 FPKM  $\geq 5$  were used as baits, and differentially expressed transcripts displaying maximum  
507 expression cutoff of  $\log_2$  transformed FPKM  $\geq 2$  were used as expression matrix. Baits and  
508 expression matrix were loaded in CoExpNetViz tool, and the analysis was run to calculate  
509 coexpression with the setting of the Pearson correlation coefficient. For the expression matrix,  
510 transcripts considered as coexpressed if their correlation does not lie between the lower (5<sup>th</sup>) and  
511 upper (95<sup>th</sup>) percentile of the distribution of correlations between a sample of genes per gene  
512 expression matrix. The output files from the CoExpNetViz tool were used for displaying gene  
513 coexpression network using Cytoscape (version 3.7.1).

#### 514 **Identification of Simple Sequence Repeats**

515 Multiple length nucleotide SSRs were identified in the transcripts of the CD-HIT-EST assembly  
516 by using the stand-alone version of Simple Sequence Repeat Identification Tool (SSRIT)  
517 (Temnykh, 2001).

518

#### 519 **Funding**

520 This work was supported by the startup funds provided to PJ by the Department of Botany and  
521 Plant Pathology in the College of Agricultural Sciences at Oregon State University. PG, MG,  
522 SN, and PJ are also supported by the National Science Foundation award IOS-1127112 and IOS  
523 -1340112.

524

525 **Disclosures**

526 The authors declare no competing interests.

527

528 **Availability of supporting data**

529 The raw sequencing data from all cDNA libraries were deposited at EMBL-EBI ArrayExpress  
530 (“ArrayExpress < EMBL-EBI”) under experiment number E-MTAB-5515.

531

532 **Figure Legends:**

533

534 **Figure 1:** Statistics of *S. hispanica* transcriptome assemblies and BLAST results. **(A)** tissue-  
535 specific assembly; **(B)** reads from each tissue types are combined and assembled at 67 k-mer and  
536 71 k-mer, Merged assembly of 67 k-mer and 71 k-mer, CD-HIT-EST and TransRate assemblies  
537 by removing redundant reads; **(C)** Comparison of *S. hispanica* transcripts with publically  
538 available Lamiales and eudicot gene models and peptide set.

539

540 **Figure 2:** Gene expression patterns across different tissues of Chia. Heatmap of hierarchical  
541 clustering of the Pearson correlations for all 13 tissues included in the gene expression atlas.  
542 Log2 transformed FPKM values were used for the similarity matrix of transcripts. The color  
543 scale indicates the degree of correlation.

544

545 **Figure 3:** Differential expression of Chia transcripts among **(A)** seed, D3-cotyledon, D3-shoot,  
546 and D12-shoot; **(B)** D12- P1 and D69- P1-P2, D69-P3-P4, D69-P5-P6-P7; **(C)** reproductive

547 stages including RacemeTop and BottomHalf tissues, D159- and D164-flowers. Vein diagrams  
548 in the upper panel represent common and unique differentially expressed transcripts in each  
549 tissue type, and scatter plots in the lower panel represent the distribution pattern of differentially  
550 expressed transcripts across each tissue type.

551  
552 **Figure 4:** Expression pattern of transcripts involved in fatty acid metabolism across tissue types.  
553 **(A)** Fatty acid metabolism; **(B)** Unsaturated fatty acids, Omega-3 ( $\alpha$ -Linolenic acid) and Omega-  
554 6 (Linoleic acid) fatty acids metabolism

555  
556 **Figure 5:** Expression pattern of transcripts involved in biosynthesis of terpenes across tissue  
557 types. Biosynthesis of IPP, a central precursor for other terpenes biosynthesis, via cytosolic  
558 MVA (mevalonate) and plastid localized MEP (2-C-methyl-D-erythritol 4-phosphate) pathways.  
559 Biosynthesis of various monoterpenes from GPP and sesquiterpenes from FPP. AACT, Acetyl-  
560 CoA acetyltransferase; HMG-CoA, 3-hydroxy-3-methylglutaryl-CoA; MVA, mevalonate;  
561 MVA-5-P, mevalonate 5-phosphate; MVAPP, mevalonate diphosphate; IPP, isopentenyl  
562 diphosphate; DMAPP, dimethylallyl diphosphate; GPP, geranyl diphosphate; FPP, farnesyl  
563 diphosphate; HMGS, HMG synthase; HMGR, HMG reductase; MK, mevalonate kinase; PMK,  
564 phosphomevalonate kinase; MDD, Mevalonate diphosphosphate decarboxylase; IPI, IPP  
565 isomerase; GPPS, geranyl diphosphate synthase; FPPS, FPP synthase; Gly-3-P, glyceraldehyde-  
566 3-phosphate; DOXP, 1- deoxy-D-xylulose-5-phosphate; MEP, 2-C-methyl-D-erythritol-4-  
567 phosphate; CDP-ME, 4-diphosphocytidyl-2-C-methyl-D-erythritol; CDP- MEP, 4-  
568 diphosphocytidyl-2-C-methyl-D-erythritol-2-phosphate; MECP, C-methyl-D-erythritol-2,4-  
569 diphosphate; HMBPP, hydroxy methylbutenyl-4-diphosphate; DXS, DOXP synthase; DXR,

570 DOXP reductoisomerase; CDP-MES, 2-C-methyl-D-erythritol4-phosphatecytidyl transferase;  
571 CDP-MEK, 4-(cytidine-5-diphospho)-2-C-methyl- D-erythritol kinase; MECPS, 2,4-C-methyl-  
572 D-erythritol cyclodiphosphate synthase; HDS, 1-hydroxy-2-methyl-2-(E)-butenyl-4-  
573 phosphatesynthase; HDR, 1-hydroxy-2-methyl-2-(E)-butenyl-4-phosphate reductase; NDH,  
574 neomenthol dehydrogenase; MS, myrcene synthase; 1,8-CS 1,8-cineole synthase; LS, linalool  
575 synthase; AHS, alpha-humulene synthase; BCS, beta-caryophyllene synthase; VS, vetispiradiene  
576 synthase; PO, premnaspirodiene oxygenase; SQ, squalene, SqS, squalene synthase; SqE,  
577 squalene epoxide; SqM, squalene monooxygenase; BAS, beta-amyrin synthase; GCS,  
578 germacrene C synthase.

579

580 **Figure 6:** Expression pattern of transcription factors and coexpression analysis with  
581 differentially expressed transcripts. **(A)** Expression pattern of differentially expressed  
582 transcription factors (633) across various developmental stages. **(B)** Coexpression network of 23  
583 highly upregulated ( $\log_2$  fold change  $\geq 5$ ) transcription factors (bait) and differentially expressed  
584 transcripts (11,055) with  $\log_2$  fold change  $\geq 2$ . Bait transcripts are shown in white color nodes  
585 with corresponding transcripts IDs, whereas correlated transcripts are represented as colored  
586 nodes. Each set of nodes is represented with different colors based on the number of correlating  
587 edges (yellow lines) connected to that node. For example- In a set of blue color nodes (1593),  
588 each transcript (blue node) showing 2 edges connected to two bait transcripts  
589 (Sh\_Salba\_v2\_130985, Sh\_Salba\_v2\_121906).

590

591 **Table 1:** Description of the plant material used for developing the Chia transcriptome Atlas.

592 Samples were collected from various developmental stages and tissue types used for

593 transcriptome analysis. DAS = Days after sowing; DAF= Days after flowering

Growth stage	Sample collection (DAS)	Sample description	Sample name
Vegetative	Day 0	Dry Seed	Seed
	Day 3	Green cotyledon	D3-Cotyledon
	Day 3	Above ground shoot parts (whole shoot)	D3-Shoot
	Day 12	Above ground shoot parts (whole shoot)	D12-Shoot
	Day 12	Very first/youngest leaf at shoot apex	D12-P1
	Day 69	First and Second leaves at the shoot apex	D69-P1-P2
	Day 69	Third and fourth leaves at the shoot apex	D69-P3-P4
	Day 69	Fifth, sixth and seventh leaves at the shoot apex	D69-P5-P6-P7
	Day 69	Internode between 6 <sup>th</sup> and 7 <sup>th</sup> leaves	D69-Internode
Reproductive	Day 158	Top half of the raceme inflorescence (pre-anthesis)	D158-RacemeTopHalf
	Day 158	Bottom half of the raceme inflorescence (pre-anthesis)	D158-RacemeBottomHalf
	Day159 (1DAF)	Flowers from 1 day after flowering (Anthesis)	D159-Flowers
	Day 164 (5DAF)	Flowers from 5 days after flowering (Anthesis)	D164-Flowers

594

595

596 **Table 2:** Differentially expressed (DE) transcripts across various developmental stages

<b>Tissue type</b>	<b>Total DE</b>	<b>Tissue specific</b>	<b>Upregulated (log<sub>2</sub> FC ≥ 2)</b>	<b>Downregulated (log<sub>2</sub> FC ≤ -2)</b>
Seed	28,641	13,450	6,284	13,429
D3-Cotyledon	7,377	1,781	2,632	1,746
D3-Shoot	3,415	495	970	1,161
D12-Shoot	2,136	270	52	1,521
D12-P1	8,795	2,038	770	3,976
D69-P1-P2	3,511	633	288	2,185
D69-P3-P4	3,019	556	479	1,701
D69-P5-P6-P7	14,140	3,504	1,884	6,637
D69-Internode	9,260	2,152	1,390	5,163
D158-RacemeTopHalf	5,591	1,183	770	2,865
D158-RacemeBottomHalf	3,614	804	852	1,860
D159-Flowers	6,047	1,136	1,274	2,883
D164-Flowers	6,134	879	969	3,353

597

598

599

600

601

602

603

604

605

606

607



608 **Table 3:** Transcripts annotated as fatty acid desaturase

<b>Fatty acid desaturases</b>	<b>Transcripts</b>
FAD2	Sh_Salba_v2_49454 Sh_Salba_v2_49451 Sh_Salba_v2_66763
FAD3	Sh_Salba_v2_74023 Sh_Salba_v2_93044 Sh_Salba_v2_93043 Sh_Salba_v2_74025 Sh_Salba_v2_93046 Sh_Salba_v2_74024 Sh_Salba_v2_74022 Sh_Salba_v2_93047 Sh_Salba_v2_93045
FAD6	Sh_Salba_v2_05727 Sh_Salba_v2_05731 Sh_Salba_v2_05730 Sh_Salba_v2_05725 Sh_Salba_v2_05728 Sh_Salba_v2_05721 Sh_Salba_v2_05724
FAD7	Sh_Salba_v2_69172
FAD8	Sh_Salba_v2_69173 Sh_Salba_v2_90850 Sh_Salba_v2_52578 Sh_Salba_v2_69162 Sh_Salba_v2_52570 Sh_Salba_v2_52575 Sh_Salba_v2_52576 Sh_Salba_v2_69169 Sh_Salba_v2_69166 Sh_Salba_v2_52573 Sh_Salba_v2_69174 Sh_Salba_v2_69171

609 **Supplementary Material**

610 **Supplementary file S1:** A summary of the raw and clean reads obtained after the sequencing  
611 and preprocessing, respectively, and reads aligned to the reference transcriptome.

612 **Supplementary file S2:** Quality assessment of merged (column 2), CD-HIT-EST (column 3)  
613 and TransRate (column 4) assemblies using QUAST

614 **Supplementary file S3:** Workflow of Chia transcriptome sequencing and downstream analysis

615 **Supplementary file S4:** Functional annotation of chia peptides using InterProScan

616 **Supplementary file S5:** Gene Ontology annotations of chia peptides

617 **Supplementary file S6:** k-means clustering of transcripts depicting tissue-specific gene  
618 expression across different developmental stages. The Y-axis in each cluster denotes the mean-  
619 centered  $\log_2$  transformed FPKM values ranging from +17 to -17.

620 **Supplementary file S7:** Transcripts clustered in 20 clusters

621 **Supplementary file S8:** Transcripts mapped to KEGG pathways

622 **Supplementary file S9:** Differentially expressed transcription factors across various  
623 developmental stages

624 **Supplementary file S10:** Frequency distribution of SSRs types in chia transcripts

625 **Supplementary file S11:** SSR motifs in chia transcripts

626 **Supplementary file S12:** SSRs identified in transcripts involved in metabolic pathways

627 **References**

- 628 Aharoni A, Jongsma MA, Bouwmeester HJ. 2005. Volatile science? Metabolic engineering of  
629 terpenoids in plants. *Trends in Plant Science* 10:594–602. DOI:  
630 10.1016/j.tplants.2005.10.005.
- 631 Ahkami A, Johnson SR, Srividya N, Lange BM. 2015a. Multiple levels of regulation determine  
632 monoterpenoid essential oil compositional variation in the mint family. *Molecular Plant*  
633 8:188–191. DOI: 10.1016/j.molp.2014.11.009.
- 634 Ahkami A, Johnson SR, Srividya N, Lange BM. 2015b. Multiple Levels of Regulation  
635 Determine Monoterpenoid Essential Oil Compositional Variation in the Mint Family.  
636 *Molecular Plant* 8:188–191. DOI: 10.1016/j.molp.2014.11.009.
- 637 Amato M, Caruso MC, Guzzo F, Galgano F, Commisso M, Bochicchio R, Labella R, Favati F.  
638 2015. Nutritional quality of seeds and leaf metabolites of Chia (*Salvia hispanica* L.) from  
639 Southern Italy. *European Food Research and Technology* 241:615–625. DOI:  
640 10.1007/s00217-015-2488-9.
- 641 Anders S, Huber W. 2010. Differential expression analysis for sequence count data. *Genome*  
642 *Biology* 11:R106. DOI: 10.1186/gb-2010-11-10-r106.
- 643 ArrayExpress < EMBL-EBI. Available at <https://www.ebi.ac.uk/arrayexpress/> (accessed  
644 December 29, 2017).
- 645 Ayerza R. 2009. The seed's protein and oil content, fatty acid composition, and growing cycle  
646 length of a single genotype of chia (*Salvia hispanica* L.) as affected by environmental  
647 factors. *Journal of Oleo Science* 58:347–354. DOI: 10.5650/jos.58.347.
- 648 Ayerza R. 2010. Effects of Seed Color and Growing Locations on Fatty Acid Content and  
649 Composition of Two Chia (*Salvia hispanica* L.) Genotypes. *Journal of the American Oil*  
650 *Chemists' Society* 87:1161–1165. DOI: 10.1007/s11746-010-1597-7.
- 651 Ayerza (h) R, Coates W. 2009. Influence of environment on growing period and yield, protein,  
652 oil and  $\alpha$ -linolenic content of three chia (*Salvia hispanica* L.) selections. *Industrial Crops*  
653 *and Products* 30:321–324. DOI: 10.1016/j.indcrop.2009.03.009.
- 654 Baginsky C, Arenas J, Escobar H, Garrido M, Valero N, Tello D, Pizarro L, Valenzuela A,  
655 Morales L, Silva H. 2016. Growth and yield of chia (*Salvia hispanica* L.) in the  
656 Mediterranean and desert climates of Chile. *Chilean journal of agricultural research*  
657 76:255–264. DOI: 10.4067/S0718-58392016000300001.

- 658 Bouajaj S, Benyamna A, Bouamama H, Romane A, Falconieri D, Piras A, Marongiu B. 2013.  
659 Antibacterial, allelopathic and antioxidant activities of essential oil of *Salvia officinalis*  
660 L. growing wild in the Atlas Mountains of Morocco. *Natural Product Research* 27:1673–  
661 1676. DOI: 10.1080/14786419.2012.751600.
- 662 Cahill JP. 2005. Human selection and domestication of chia (*salvia hispanica* l.). *Journal of*  
663 *Ethnobiology* 25:155–174. DOI: 10.2993/0278-0771(2005)25[155:HSADOC]2.0.CO;2.
- 664 Cai S, Lashbrook CC. 2008. Stamen abscission zone transcriptome profiling reveals new  
665 candidates for abscission control: enhanced retention of floral organs in transgenic plants  
666 overexpressing *Arabidopsis* ZINC FINGER PROTEIN2. *Plant Physiology* 146:1305–  
667 1321. DOI: 10.1104/pp.107.110908.
- 668 Cañas RA, Li Z, Pascual MB, Castro-Rodríguez V, Ávila C, Sterck L, Van de Peer Y, Cánovas  
669 FM. 2017. The gene expression landscape of pine seedling tissues. *The Plant Journal:*  
670 *For Cell and Molecular Biology* 91:1064–1087. DOI: 10.1111/tbj.13617.
- 671 Cassan-Wang H, Goué N, Saidi MN, Legay S, Sivadon P, Goffner D, Grima-Pettenati J. 2013.  
672 Identification of novel transcription factors regulating secondary cell wall formation in  
673 *Arabidopsis*. *Frontiers in Plant Science* 4:189. DOI: 10.3389/fpls.2013.00189.
- 674 Chicco AG, D'Alessandro ME, Hein GJ, Oliva ME, Lombardo YB. 2009. Dietary chia seed (  
675 *Salvia hispanica* L.) rich in  $\alpha$ -linolenic acid improves adiposity and normalises  
676 hypertriacylglycerolaemia and insulin resistance in dyslipaemic rats. *British Journal of*  
677 *Nutrition* 101:41–50. DOI: 10.1017/S000711450899053X.
- 678 Clevenger J, Chu Y, Scheffler B, Ozias-Akins P. 2016. A Developmental Transcriptome Map for  
679 Allotetraploid *Arachis hypogaea*. *Frontiers in Plant Science* 7:1446. DOI:  
680 10.3389/fpls.2016.01446.
- 681 Cui G, Duan L, Jin B, Qian J, Xue Z, Shen G, Snyder JH, Song J, Chen S, Huang L, Peters RJ,  
682 Qi X. 2015. Functional Divergence of Diterpene Syntheses in the Medicinal Plant *Salvia*  
683 *miltiorrhiza*. *Plant Physiology* 169:1607–1618. DOI: 10.1104/pp.15.00695.
- 684 Dar AA, Choudhury AR, Kancharla PK, Arumugam N. 2017. The FAD2 Gene in Plants:  
685 Occurrence, Regulation, and Role. *Frontiers in Plant Science* 8:1789. DOI:  
686 10.3389/fpls.2017.01789.
- 687 Druka A, Muehlbauer G, Druka I, Caldo R, Baumann U, Rostoks N, Schreiber A, Wise R, Close  
688 T, Kleinhofs A, Graner A, Schulman A, Langridge P, Sato K, Hayes P, McNicol J,

- 689 Marshall D, Waugh R. 2006. An atlas of gene expression from seed to seed through  
690 barley development. *Functional & Integrative Genomics* 6:202–211. DOI:  
691 10.1007/s10142-006-0025-4.
- 692 Du Z, Zhou X, Ling Y, Zhang Z, Su Z. 2010a. agriGO: a GO analysis toolkit for the agricultural  
693 community. *Nucleic Acids Research* 38:W64-70. DOI: 10.1093/nar/gkq310.
- 694 Du Z, Zhou X, Ling Y, Zhang Z, Su Z. 2010b. agriGO: a GO analysis toolkit for the agricultural  
695 community. *Nucleic Acids Research* 38:W64–W70. DOI: 10.1093/nar/gkq310.
- 696 Elshafie HS, Aliberti L, Amato M, De Feo V, Camele I. 2018. Chemical composition and  
697 antimicrobial activity of chia (*Salvia hispanica* L.) essential oil. *European Food Research*  
698 *and Technology* 244:1675–1682. DOI: 10.1007/s00217-018-3080-x.
- 699 Ge X, Chen H, Wang H, Shi A, Liu K. 2014. De Novo Assembly and Annotation of *Salvia*  
700 *splendens* Transcriptome Using the Illumina Platform. *PLoS ONE* 9. DOI:  
701 10.1371/journal.pone.0087693.
- 702 Gomez MD, Urbez C, Perez-Amador MA, Carbonell J. 2011. Characterization of constricted  
703 fruit (ctf) mutant uncovers a role for AtMYB117/LOF1 in ovule and fruit development in  
704 *Arabidopsis thaliana*. *PLoS One* 6:e18760. DOI: 10.1371/journal.pone.0018760.
- 705 Gómez-Ariza J, Brambilla V, Vicentini G, Landini M, Cerise M, Carrera E, Shrestha R,  
706 Chiozzotto R, Galbiati F, Caporali E, López Díaz I, Fornara F. 2019. A transcription  
707 factor coordinating internode elongation and photoperiodic signals in rice. *Nature Plants*  
708 5:358–362. DOI: 10.1038/s41477-019-0401-4.
- 709 Gould J.GENE-E. Available at <https://software.broadinstitute.org/GENE-E/index.html> (accessed  
710 April 10, 2017).
- 711 Grant EH, Fujino T, Beers EP, Brunner AM. 2010. Characterization of NAC domain  
712 transcription factors implicated in control of vascular cell differentiation in *Arabidopsis*  
713 and *Populus*. *Planta* 232:337–352. DOI: 10.1007/s00425-010-1181-2.
- 714 Guo H, Li L, Ye H, Yu X, Algreen A, Yin Y. 2009. Three related receptor-like kinases are  
715 required for optimal cell elongation in *Arabidopsis thaliana*. *Proceedings of the National*  
716 *Academy of Sciences of the United States of America* 106:7648–7653. DOI:  
717 10.1073/pnas.0812346106.
- 718 Gurevich A, Saveliev V, Vyahhi N, Tesler G. 2013. QUAST: quality assessment tool for genome  
719 assemblies. *Bioinformatics* 29:1072–1075. DOI: 10.1093/bioinformatics/btt086.

- 720 Haruta M, Sabat G, Stecker K, Minkoff BB, Sussman MR. 2014. A peptide hormone and its  
721 receptor protein kinase regulate plant cell expansion. *Science (New York, N.Y.)* 343:408–  
722 411. DOI: 10.1126/science.1244454.
- 723 Horiguchi G, Kim G-T, Tsukaya H. 2005. The transcription factor AtGRF5 and the transcription  
724 coactivator AN3 regulate cell proliferation in leaf primordia of *Arabidopsis thaliana*. *The*  
725 *Plant Journal: For Cell and Molecular Biology* 43:68–78. DOI: 10.1111/j.1365-  
726 313X.2005.02429.x.
- 727 Imran M, Nadeem M, Manzoor MF, Javed A, Ali Z, Akhtar MN, Ali M, Hussain Y. 2016. Fatty  
728 acids characterization, oxidative perspectives and consumer acceptability of oil extracted  
729 from pre-treated chia (*Salvia hispanica* L.) seeds. *Lipids in Health and Disease* 15:162.  
730 DOI: 10.1186/s12944-016-0329-x.
- 731 Ixtaina VY, Nolasco SM, Tomás MC. 2008. Physical properties of chia (*Salvia hispanica* L.)  
732 seeds. *Industrial Crops and Products* 28:286–293. DOI: 10.1016/j.indcrop.2008.03.009.
- 733 Jin J, Tian F, Yang D-C, Meng Y-Q, Kong L, Luo J, Gao G. 2017. PlantTFDB 4.0: toward a  
734 central hub for transcription factors and regulatory interactions in plants. *Nucleic Acids*  
735 *Research* 45:D1040–D1045. DOI: 10.1093/nar/gkw982.
- 736 Jones P, Binns D, Chang H-Y, Fraser M, Li W, McAnulla C, McWilliam H, Maslen J, Mitchell  
737 A, Nuka G, Pesseat S, Quinn AF, Sangrador-Vegas A, Scheremetjew M, Yong S-Y,  
738 Lopez R, Hunter S. 2014a. InterProScan 5: genome-scale protein function classification.  
739 *Bioinformatics (Oxford, England)* 30:1236–1240. DOI: 10.1093/bioinformatics/btu031.
- 740 Jones P, Binns D, Chang H-Y, Fraser M, Li W, McAnulla C, McWilliam H, Maslen J, Mitchell  
741 A, Nuka G, Pesseat S, Quinn AF, Sangrador-Vegas A, Scheremetjew M, Yong S-Y,  
742 Lopez R, Hunter S. 2014b. InterProScan 5: genome-scale protein function classification.  
743 *Bioinformatics* 30:1236–1240. DOI: 10.1093/bioinformatics/btu031.
- 744 Jones SI, Vodkin LO. 2013. Using RNA-Seq to profile soybean seed development from  
745 fertilization to maturity. *PloS One* 8:e59270. DOI: 10.1371/journal.pone.0059270.
- 746 Joyce BL, Haug-Baltzell AK, Hulvey JP, McCarthy F, Devisetty UK, Lyons E. 2017.  
747 Leveraging CyVerse Resources for De Novo Comparative Transcriptomics of  
748 Underserved (Non-model) Organisms. *JoVE (Journal of Visualized*  
749 *Experiments)*:e55009–e55009. DOI: 10.3791/55009.

- 750 Juergens UR. 2014. Anti-inflammatory properties of the monoterpene 1.8-cineole: current  
751 evidence for co-medication in inflammatory airway diseases. *Drug Research* 64:638–  
752 646. DOI: 10.1055/s-0034-1372609.
- 753 Kagale S, Nixon J, Khedikar Y, Pasha A, Provart NJ, Clarke WE, Bollina V, Robinson SJ, Coutu  
754 C, Hegedus DD, Sharpe AG, Parkin IAP. 2016. The developmental transcriptome atlas of  
755 the biofuel crop *Camelina sativa*. *The Plant Journal: For Cell and Molecular Biology*  
756 88:879–894. DOI: 10.1111/tpj.13302.
- 757 Kebrom TH, McKinley B, Mullet JE. 2017. Dynamics of gene expression during development  
758 and expansion of vegetative stem internodes of bioenergy sorghum. *Biotechnology for*  
759 *Biofuels* 10:159. DOI: 10.1186/s13068-017-0848-3.
- 760 Khedher MRB, Khedher SB, Chaieb I, Tounsi S, Hammami M. 2017. Chemical composition and  
761 biological activities of *Salvia officinalis* essential oil from Tunisia. *EXCLI Journal*  
762 16:160–173. DOI: 10.17179/excli2016-832.
- 763 Kim JH, Choi D, Kende H. 2003. The AtGRF family of putative transcription factors is involved  
764 in leaf and cotyledon growth in *Arabidopsis*. *The Plant Journal: For Cell and Molecular*  
765 *Biology* 36:94–104.
- 766 Kobayashi K, Suzuki T, Iwata E, Nakamichi N, Suzuki T, Chen P, Ohtani M, Ishida T, Hosoya  
767 H, Müller S, Leviczky T, Pettkó-Szandtner A, Darula Z, Iwamoto A, Nomoto M, Tada Y,  
768 Higashiyama T, Demura T, Doonan JH, Hauser M-T, Sugimoto K, Umeda M, Magyar Z,  
769 Bögre L, Ito M. 2015. Transcriptional repression by MYB3R proteins regulates plant  
770 organ growth. *The EMBO journal* 34:1992–2007. DOI: 10.15252/embj.201490899.
- 771 Kudapa H, Garg V, Chitkineni A, Varshney RK. 2018. The RNA-Seq-based high resolution  
772 gene expression atlas of chickpea (*Cicer arietinum* L.) reveals dynamic spatio-temporal  
773 changes associated with growth and development. *Plant, Cell & Environment* 41:2209–  
774 2225. DOI: 10.1111/pce.13210.
- 775 Langmead B, Salzberg SL. 2012. Fast gapped-read alignment with Bowtie 2. *Nature Methods*  
776 9:357–359. DOI: 10.1038/nmeth.1923.
- 777 Lee BH, Ko J-H, Lee S, Lee Y, Pak J-H, Kim JH. 2009. The *Arabidopsis* GRF-INTERACTING  
778 FACTOR gene family performs an overlapping function in determining organ size as  
779 well as multiple developmental properties. *Plant Physiology* 151:655–668. DOI:  
780 10.1104/pp.109.141838.



- 781 Leng N, Dawson JA, Thomson JA, Ruotti V, Rissman AI, Smits BMG, Haag JD, Gould MN,  
782 Stewart RM, Kendzierski C. 2013. EBSeq: an empirical Bayes hierarchical model for  
783 inference in RNA-seq experiments. *Bioinformatics*:btt087. DOI:  
784 10.1093/bioinformatics/btt087.
- 785 Li B, Dewey CN. 2011a. RSEM: accurate transcript quantification from RNA-Seq data with or  
786 without a reference genome. *BMC Bioinformatics* 12:323. DOI: 10.1186/1471-2105-12-  
787 323.
- 788 Li B, Dewey CN. 2011b. RSEM: accurate transcript quantification from RNA-Seq data with or  
789 without a reference genome. *BMC Bioinformatics* 12:323. DOI: 10.1186/1471-2105-12-  
790 323.
- 791 Li W, Godzik A. 2006. Cd-hit: a fast program for clustering and comparing large sets of protein  
792 or nucleotide sequences. *Bioinformatics* 22:1658–1659. DOI:  
793 10.1093/bioinformatics/btl158.
- 794 Libault M, Farmer A, Joshi T, Takahashi K, Langley RJ, Franklin LD, He J, Xu D, May G,  
795 Stacey G. 2010. An integrated transcriptome atlas of the crop model Glycine max, and its  
796 use in comparative analyses in plants. *The Plant Journal: For Cell and Molecular*  
797 *Biology* 63:86–99. DOI: 10.1111/j.1365-313X.2010.04222.x.
- 798 Liu X, Qin T, Ma Q, Sun J, Liu Z, Yuan M, Mao T. 2013. Light-regulated hypocotyl elongation  
799 involves proteasome-dependent degradation of the microtubule regulatory protein WDL3  
800 in Arabidopsis. *The Plant Cell* 25:1740–1755. DOI: 10.1105/tpc.113.112789.
- 801 Ma Y, Yuan L, Wu B, Li X, Chen S, Lu S. 2012. Genome-wide identification and  
802 characterization of novel genes involved in terpenoid biosynthesis in *Salvia miltiorrhiza*.  
803 *Journal of Experimental Botany*:err466. DOI: 10.1093/jxb/err466.
- 804 Manosalva PM, Davidson RM, Liu B, Zhu X, Hulbert SH, Leung H, Leach JE. 2009. A germin-  
805 like protein gene family functions as a complex quantitative trait locus conferring broad-  
806 spectrum disease resistance in rice. *Plant Physiology* 149:286–296. DOI:  
807 10.1104/pp.108.128348.
- 808 Marcinek K, Krejpcio Z. 2017. Chia seeds (*Salvia hispanica*): health promoting properties and  
809 therapeutic applications – a review. *Roczniki Panstwowego Zakladu Higieny* 68:123–129.  
810 *mev: MultiExperiment Viewer*. 2017. CCCB at Dana-Farber Cancer Institute.



- 811 Mikheenko A, Valin G, Prjibelski A, Saveliev V, Gurevich A. 2016. Icarus: visualizer for de  
812 novo assembly evaluation. *Bioinformatics (Oxford, England)*. DOI:  
813 10.1093/bioinformatics/btw379.
- 814 Millar AA, Gubler F. 2005. The Arabidopsis GAMYB-like genes, MYB33 and MYB65, are  
815 microRNA-regulated genes that redundantly facilitate anther development. *The Plant*  
816 *Cell* 17:705–721. DOI: 10.1105/tpc.104.027920.
- 817 Mohd Ali N, Yeap SK, Ho WY, Beh BK, Tan SW, Tan SG. 2012. The Promising Future of  
818 Chia, *Salvia hispanica* L. *BioMed Research International* 2012. DOI:  
819 10.1155/2012/171956.
- 820 Moriya Y, Itoh M, Okuda S, Yoshizawa AC, Kanehisa M. 2007. KAAS: an automatic genome  
821 annotation and pathway reconstruction server. *Nucleic Acids Research* 35:W182-185.  
822 DOI: 10.1093/nar/gkm321.
- 823 Moss M, Oliver L. 2012. Plasma 1,8-cineole correlates with cognitive performance following  
824 exposure to rosemary essential oil aroma. *Therapeutic Advances in Psychopharmacology*  
825 2:103–113. DOI: 10.1177/2045125312436573.
- 826 Mount DW. 2007. Using the Basic Local Alignment Search Tool (BLAST). *Cold Spring Harbor*  
827 *Protocols* 2007:pdb.top17. DOI: 10.1101/pdb.top17.
- 828 Muñoz LA, Cobos A, Diaz O, Aguilera JM. 2013. Chia Seed (*Salvia hispanica*): An Ancient  
829 Grain and a New Functional Food. *Food Reviews International* 29:394–408. DOI:  
830 10.1080/87559129.2013.818014.
- 831 najoshi/sickle. Available at <https://github.com/najoshi/sickle> (accessed June 6, 2014).
- 832 Nakashima K, Shinwari ZK, Sakuma Y, Seki M, Miura S, Shinozaki K, Yamaguchi-Shinozaki  
833 K. 2000. Organization and expression of two Arabidopsis DREB2 genes encoding DRE-  
834 binding proteins involved in dehydration- and high-salinity-responsive gene expression.  
835 *Plant Molecular Biology* 42:657–665. DOI: 10.1023/a:1006321900483.
- 836 Nath U, Crawford BCW, Carpenter R, Coen E. 2003. Genetic Control of Surface Curvature.  
837 *Science* 299:1404–1407. DOI: 10.1126/science.1079354.
- 838 Nishimura C, Ohashi Y, Sato S, Kato T, Tabata S, Ueguchi C. 2004. Histidine kinase homologs  
839 that act as cytokinin receptors possess overlapping functions in the regulation of shoot  
840 and root growth in Arabidopsis. *The Plant Cell* 16:1365–1377. DOI: 10.1105/tpc.021477.

- 841 Oliva ME, Ferreira MR, Chicco A, Lombardo YB. 2013. Dietary Salba (*Salvia hispanica* L.) seed  
842 rich in  $\alpha$ -linolenic acid improves adipose tissue dysfunction and the altered skeletal  
843 muscle glucose and lipid metabolism in dyslipidemic insulin-resistant rats.  
844 *Prostaglandins, Leukotrienes and Essential Fatty Acids (PLEFA)* 89:279–289. DOI:  
845 10.1016/j.plefa.2013.09.010.
- 846 Patro R, Duggal G, Love MI, Irizarry RA, Kingsford C. 2017. Salmon provides fast and bias-  
847 aware quantification of transcript expression. *Nature Methods* 14:417–419. DOI:  
848 10.1038/nmeth.4197.
- 849 Peiretti PG, Gai F. 2009. Fatty acid and nutritive quality of chia (*Salvia hispanica* L.) seeds and  
850 plant during growth. *Animal Feed Science and Technology* 148:267–275. DOI:  
851 10.1016/j.anifeedsci.2008.04.006.
- 852 Peláez P, Orona-Tamayo D, Montes-Hernández S, Valverde ME, Paredes-López O, Cibrián-  
853 Jaramillo A. 2019. Comparative transcriptome analysis of cultivated and wild seeds of  
854 *Salvia hispanica* (chia). *Scientific Reports* 9:9761. DOI: 10.1038/s41598-019-45895-5.
- 855 R. V. S, Kumari P, Rupwate SD, Rajasekharan R, Srinivasan M. 2015. Exploring Triacylglycerol  
856 Biosynthetic Pathway in Developing Seeds of Chia (*Salvia hispanica* L.): A  
857 Transcriptomic Approach. *PLoS ONE* 10. DOI: 10.1371/journal.pone.0123580.
- 858 Reeves PH, Ellis CM, Ploense SE, Wu M-F, Yadav V, Tholl D, Chételat A, Haupt I, Kennerley  
859 BJ, Hodgens C, Farmer EE, Nagpal P, Reed JW. 2012. A regulatory network for  
860 coordinated flower maturation. *PLoS genetics* 8:e1002506. DOI:  
861 10.1371/journal.pgen.1002506.
- 862 Reyes-Caudillo E, Tecante A, Valdivia-López MA. 2008. Dietary fibre content and antioxidant  
863 activity of phenolic compounds present in Mexican chia (*Salvia hispanica* L.) seeds.  
864 *Food Chemistry* 107:656–663. DOI: 10.1016/j.foodchem.2007.08.062.
- 865 Robinson MD, McCarthy DJ, Smyth GK. 2010. edgeR: a Bioconductor package for differential  
866 expression analysis of digital gene expression data. *Bioinformatics (Oxford, England)*  
867 26:139–140. DOI: 10.1093/bioinformatics/btp616.
- 868 Rogers HJ. 2012. Is there an important role for reactive oxygen species and redox regulation  
869 during floral senescence? *Plant, Cell & Environment* 35:217–233. DOI: 10.1111/j.1365-  
870 3040.2011.02373.x.

- 871 Rogers H, Munné-Bosch S. 2016. Production and Scavenging of Reactive Oxygen Species and  
872 Redox Signaling during Leaf and Flower Senescence: Similar But Different1[OPEN].  
873 *Plant Physiology* 171:1560–1568. DOI: 10.1104/pp.16.00163.
- 874 Sakuma Y, Liu Q, Dubouzet JG, Abe H, Shinozaki K, Yamaguchi-Shinozaki K. 2002. DNA-  
875 binding specificity of the ERF/AP2 domain of Arabidopsis DREBs, transcription factors  
876 involved in dehydration- and cold-inducible gene expression. *Biochemical and*  
877 *Biophysical Research Communications* 290:998–1009. DOI: 10.1006/bbrc.2001.6299.
- 878 Schulz MH, Zerbino DR, Vingron M, Birney E. 2012. Oases: robust de novo RNA-seq assembly  
879 across the dynamic range of expression levels. *Bioinformatics* 28:1086–1092. DOI:  
880 10.1093/bioinformatics/bts094.
- 881 Sekhon RS, Lin H, Childs KL, Hansey CN, Buell CR, de Leon N, Kaeppler SM. 2011. Genome-  
882 wide atlas of transcription during maize development. *The Plant Journal: For Cell and*  
883 *Molecular Biology* 66:553–563. DOI: 10.1111/j.1365-313X.2011.04527.x.
- 884 Severin AJ, Woody JL, Bolon Y-T, Joseph B, Diers BW, Farmer AD, Muehlbauer GJ, Nelson  
885 RT, Grant D, Specht JE, Graham MA, Cannon SB, May GD, Vance CP, Shoemaker RC.  
886 2010. RNA-Seq Atlas of Glycine max: a guide to the soybean transcriptome. *BMC plant*  
887 *biology* 10:160. DOI: 10.1186/1471-2229-10-160.
- 888 Shpak ED, McAbee JM, Pillitteri LJ, Torii KU. 2005. Stomatal patterning and differentiation by  
889 synergistic interactions of receptor kinases. *Science (New York, N.Y.)* 309:290–293. DOI:  
890 10.1126/science.1109710.
- 891 Sibout R, Eudes A, Mouille G, Pollet B, Lapierre C, Jouanin L, Séguin A. 2005. CINNAMYL  
892 ALCOHOL DEHYDROGENASE-C and -D are the primary genes involved in lignin  
893 biosynthesis in the floral stem of Arabidopsis. *The Plant Cell* 17:2059–2076. DOI:  
894 10.1105/tpc.105.030767.
- 895 Singh R, Singh S, Parihar P, Mishra RK, Tripathi DK, Singh VP, Chauhan DK, Prasad SM.  
896 2016. Reactive Oxygen Species (ROS): Beneficial Companions of Plants’ Developmental  
897 Processes. *Frontiers in Plant Science* 7. DOI: 10.3389/fpls.2016.01299.
- 898 Smith-Unna R, Bournnell C, Patro R, Hibberd J, Kelly S. 2016. TransRate: reference free quality  
899 assessment of de novo transcriptome assemblies. *Genome Research*:gr.196469.115. DOI:  
900 10.1101/gr.196469.115.

- 901 Sreeharsha RV, Mudalkar S, Singha KT, Reddy AR. 2016. Unravelling molecular mechanisms  
902 from floral initiation to lipid biosynthesis in a promising biofuel tree species, *Pongamia*  
903 *pinnata* using transcriptome analysis. *Scientific Reports* 6. DOI: 10.1038/srep34315.
- 904 Stelpflug SC, Sekhon RS, Vaillancourt B, Hirsch CN, Buell CR, de Leon N, Kaeppler SM. 2016.  
905 An Expanded Maize Gene Expression Atlas based on RNA Sequencing and its Use to  
906 Explore Root Development. *The Plant Genome* 9. DOI:  
907 10.3835/plantgenome2015.04.0025.
- 908 Tan J, Jin M, Wang J, Wu F, Sheng P, Cheng Z, Wang J, Zheng X, Chen L, Wang M, Zhu S,  
909 Guo X, Zhang X, Liu X, Wang C, Wang H, Wu C, Wan J. 2016. OsCOL10, a  
910 CONSTANS-Like Gene, Functions as a Flowering Time Repressor Downstream of Ghd7  
911 in Rice. *Plant & Cell Physiology* 57:798–812. DOI: 10.1093/pcp/pcw025.
- 912 Temnykh S. 2001. Computational and Experimental Analysis of Microsatellites in Rice (*Oryza*  
913 *sativa* L.): Frequency, Length Variation, Transposon Associations, and Genetic Marker  
914 Potential. *Genome Research* 11:1441–1452. DOI: 10.1101/gr.184001.
- 915 TransDecoder (Find Coding Regions Within Transcripts). Available at  
916 [https://transdecoder.github.io/#incl\\_homology](https://transdecoder.github.io/#incl_homology) (accessed January 23, 2017).
- 917 Triikka FA, Nikolaidis A, Ignea C, Tsaballa A, Tziveleka L-A, Ioannou E, Roussis V, Stea EA,  
918 Božić D, Argiriou A, Kanellis AK, Kampranis SC, Makris AM. 2015. Combined  
919 metabolome and transcriptome profiling provides new insights into diterpene  
920 biosynthesis in *S. pomifera* glandular trichomes. *BMC Genomics* 16:935. DOI:  
921 10.1186/s12864-015-2147-3.
- 922 Tzfadia O, Diels T, De Meyer S, Vandepoele K, Aharoni A, Van de Peer Y. 2015.  
923 CoExpNetViz: Comparative Co-Expression Networks Construction and Visualization  
924 Tool. *Frontiers in Plant Science* 6:1194. DOI: 10.3389/fpls.2015.01194.
- 925 Ueguchi C, Sato S, Kato T, Tabata S. 2001. The AHK4 gene involved in the cytokinin-signaling  
926 pathway as a direct receptor molecule in *Arabidopsis thaliana*. *Plant & Cell Physiology*  
927 42:751–755. DOI: 10.1093/pcp/pce094.
- 928 Ullah R, Nadeem M, Khaliq A, Imran M, Mehmood S, Javid A, Hussain J. 2016. Nutritional  
929 and therapeutic perspectives of Chia (*Salvia hispanica* L.): a review. *Journal of Food*  
930 *Science and Technology* 53:1750–1758. DOI: 10.1007/s13197-015-1967-0.

- 931 Valdivia-López MÁ, Tecante A. 2015. Chia (*Salvia hispanica*): A Review of Native Mexican  
932 Seed and its Nutritional and Functional Properties. *Advances in Food and Nutrition*  
933 *Research* 75:53–75. DOI: 10.1016/bs.afnr.2015.06.002.
- 934 do Vale TG, Furtado EC, Santos JG, Viana GSB. 2002. Central effects of citral, myrcene and  
935 limonene, constituents of essential oil chemotypes from *Lippia alba* (Mill.) n.e. Brown.  
936 *Phytomedicine: International Journal of Phytotherapy and Phytopharmacology* 9:709–  
937 714.
- 938 Vuksan V, Choleva L, Jovanovski E, Jenkins AL, Au-Yeung F, Dias AG, Ho HVT, Zurbau A,  
939 Duvnjak L. 2017a. Comparison of flax (*Linum usitatissimum*) and Salba-chia (*Salvia*  
940 *hispanica* L.) seeds on postprandial glycemia and satiety in healthy individuals: a  
941 randomized, controlled, crossover study. *European Journal of Clinical Nutrition* 71:234–  
942 238. DOI: 10.1038/ejcn.2016.148.
- 943 Vuksan V, Jenkins AL, Brissette C, Choleva L, Jovanovski E, Gibbs AL, Bazinet RP, Au-Yeung  
944 F, Zurbau A, Ho HVT, Duvnjak L, Sievenpiper JL, Josse RG, Hanna A. 2017b. Salba-  
945 chia (*Salvia hispanica* L.) in the treatment of overweight and obese patients with type 2  
946 diabetes: A double-blind randomized controlled trial. *Nutrition, metabolism, and*  
947 *cardiovascular diseases: NMCD* 27:138–146. DOI: 10.1016/j.numecd.2016.11.124.
- 948 Vuksan V, Jenkins AL, Dias AG, Lee AS, Jovanovski E, Rogovik AL, Hanna A. 2010.  
949 Reduction in postprandial glucose excursion and prolongation of satiety: possible  
950 explanation of the long-term effects of whole grain Salba (*Salvia Hispanica* L.).  
951 *European journal of clinical nutrition* 64:436–438.
- 952 Vuksan V, Whitham D, Sievenpiper JL, Jenkins AL, Rogovik AL, Bazinet RP, Vidgen E, Hanna  
953 A. 2007. Supplementation of conventional therapy with the novel grain Salba (*Salvia*  
954 *hispanica* L.) improves major and emerging cardiovascular risk factors in type 2 diabetes:  
955 results of a randomized controlled trial. *Diabetes care* 30:2804–2810. DOI:  
956 10.2337/dc07-1144.
- 957 Wang T, Chen X, Zhu F, Li H, Li L, Yang Q, Chi X, Yu S, Liang X. 2013. Characterization of  
958 peanut germin-like proteins, AhGLPs in plant development and defense. *PloS One*  
959 8:e61722. DOI: 10.1371/journal.pone.0061722.

- 960 Wenping H, Yuan Z, Jie S, Lijun Z, Zhezhi W. 2011. De novo transcriptome sequencing in  
961 *Salvia miltiorrhiza* to identify genes involved in the biosynthesis of active ingredients.  
962 *Genomics* 98:272–279. DOI: 10.1016/j.ygeno.2011.03.012.
- 963 Wolf C, Hennig M, Romanovicz D, Steinebrunner I. 2007. Developmental defects and seedling  
964 lethality in apyrase AtAPY1 and AtAPY2 double knockout mutants. *Plant Molecular*  
965 *Biology* 64:657–672. DOI: 10.1007/s11103-007-9184-5.
- 966 Xue Y, Chen B, Win AN, Fu C, Lian J, Liu X, Wang R, Zhang X, Chai Y. 2018. Omega-3 fatty  
967 acid desaturase gene family from two  $\omega$ -3 sources, *Salvia hispanica* and *Perilla*  
968 *frutescens*: Cloning, characterization and expression. *PLoS ONE* 13. DOI:  
969 10.1371/journal.pone.0191432.
- 970 Yang C, Xu Z, Song J, Conner K, Vizcay Barrena G, Wilson ZA. 2007. Arabidopsis  
971 MYB26/MALE STERILE35 regulates secondary thickening in the endothecium and is  
972 essential for anther dehiscence. *The Plant Cell* 19:534–548. DOI:  
973 10.1105/tpc.106.046391.
- 974 Zdobnov EM, Apweiler R. 2001a. InterProScan--an integration platform for the signature-  
975 recognition methods in InterPro. *Bioinformatics (Oxford, England)* 17:847–848. DOI:  
976 10.1093/bioinformatics/17.9.847.
- 977 Zdobnov EM, Apweiler R. 2001b. InterProScan – an integration platform for the signature-  
978 recognition methods in InterPro. *Bioinformatics* 17:847–848. DOI:  
979 10.1093/bioinformatics/17.9.847.
- 980 Zerbino DR, Birney E. 2008. Velvet: Algorithms for de novo short read assembly using de  
981 Bruijn graphs. *Genome Research* 18:821–829. DOI: 10.1101/gr.074492.107.
- 982 Zhang J, Liu H, Sun J, Li B, Zhu Q, Chen S, Zhang H. 2012. Arabidopsis Fatty Acid Desaturase  
983 FAD2 Is Required for Salt Tolerance during Seed Germination and Early Seedling  
984 Growth. *PLOS ONE* 7:e30355. DOI: 10.1371/journal.pone.0030355.
- 985 Zhang H, Miao H, Wang L, Qu L, Liu H, Wang Q, Yue M. 2013. Genome sequencing of the  
986 important oilseed crop *Sesamum indicum*L. *Genome Biology* 14:401. DOI: 10.1186/gb-  
987 2013-14-1-401.
- 988 Zhong R, Lee C, Zhou J, McCarthy RL, Ye Z-H. 2008. A battery of transcription factors  
989 involved in the regulation of secondary cell wall biosynthesis in Arabidopsis. *The Plant*  
990 *Cell* 20:2763–2782. DOI: 10.1105/tpc.108.061325.

- 991 Zimmermann G, Bäumlein H, Mock H-P, Himmelbach A, Schweizer P. 2006. The multigene  
992 family encoding germin-like proteins of barley. Regulation and function in Basal host  
993 resistance. *Plant Physiology* 142:181–192. DOI: 10.1104/pp.106.083824.
- 994 Zimmermann IM, Heim MA, Weisshaar B, Uhrig JF. 2004. Comprehensive identification of  
995 *Arabidopsis thaliana* MYB transcription factors interacting with R/B-like BHLH proteins.  
996 *The Plant Journal: For Cell and Molecular Biology* 40:22–34. DOI: 10.1111/j.1365-  
997 313X.2004.02183.x.
- 998



**Figure 1**

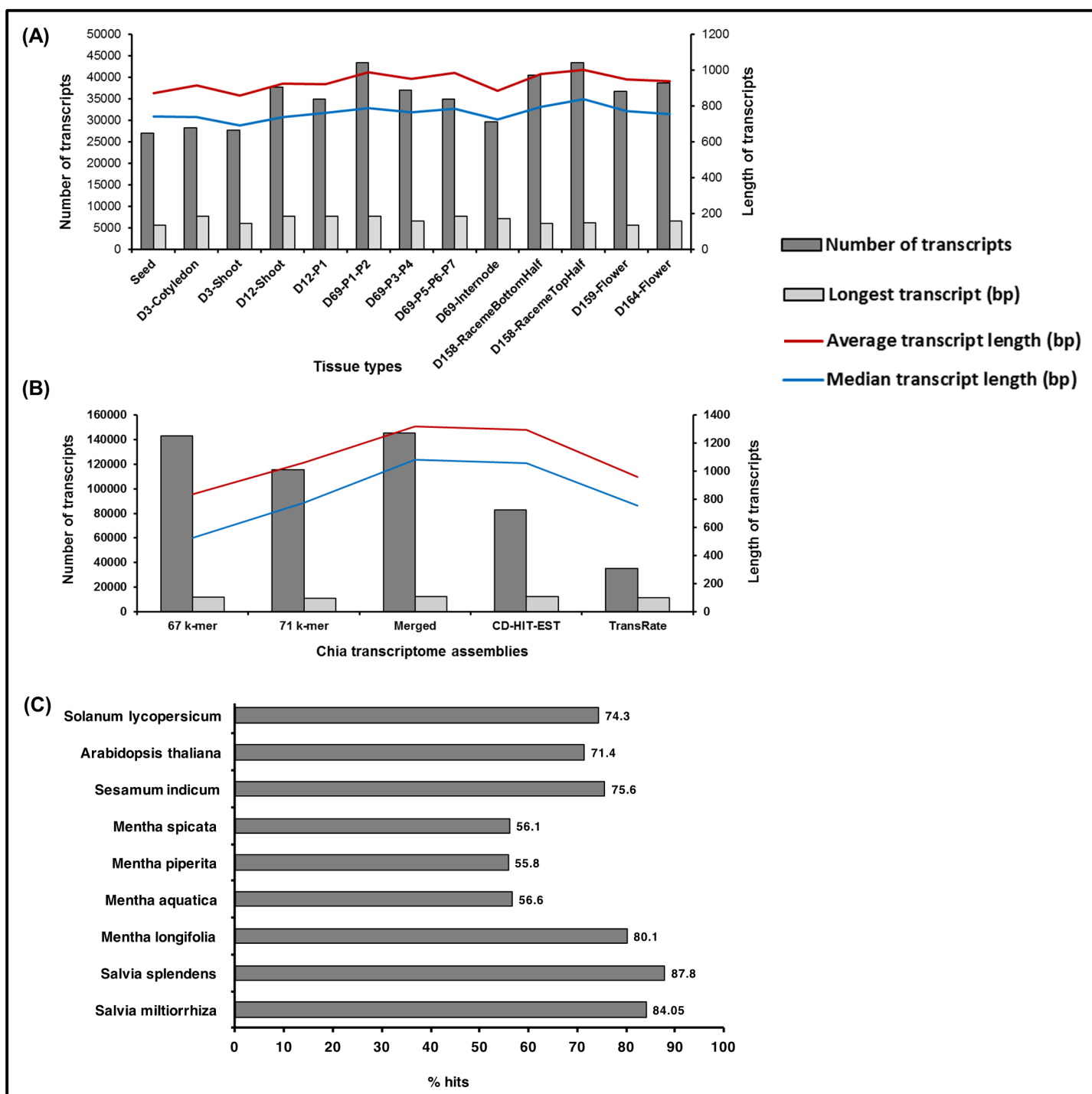




Figure 2

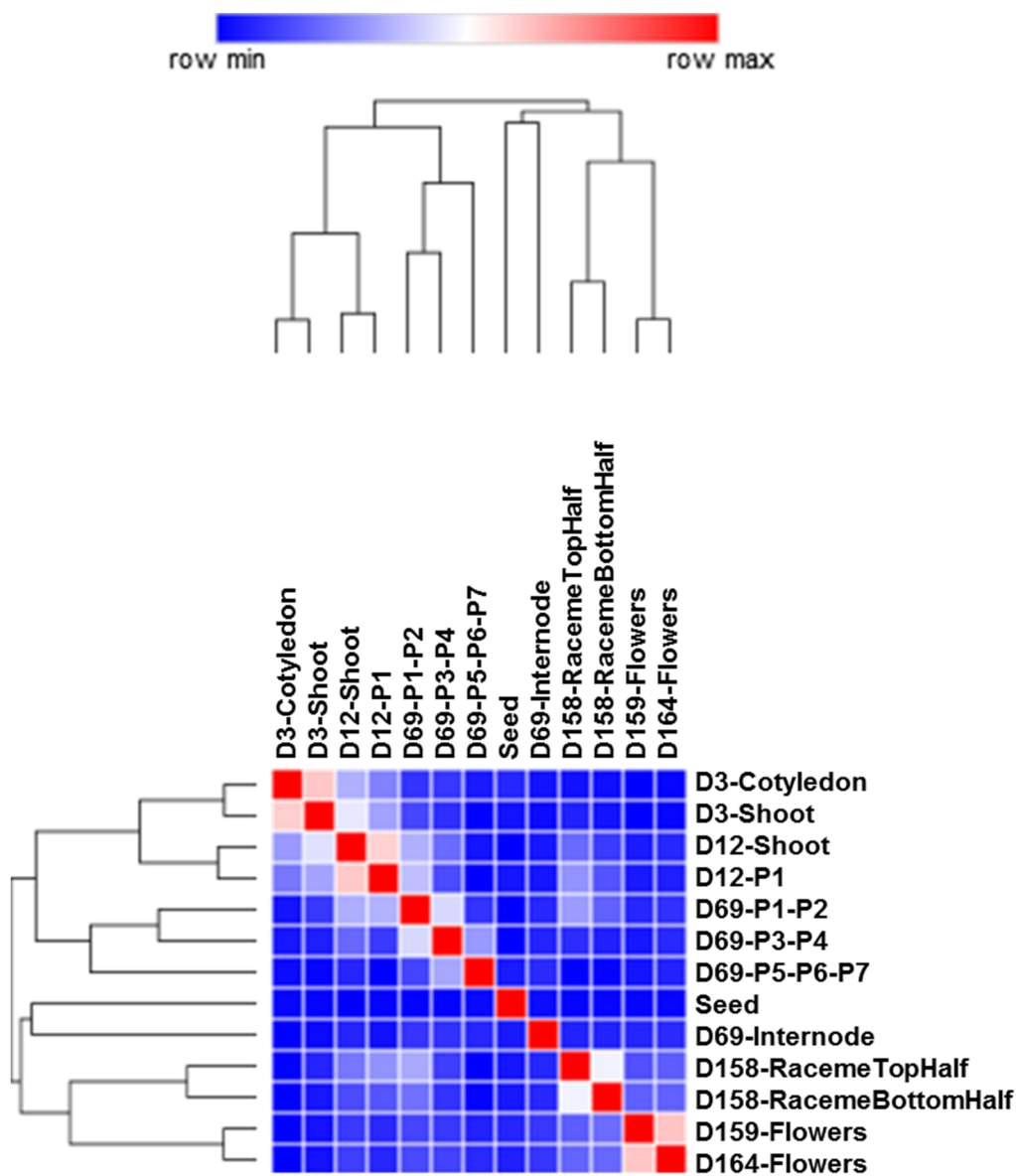
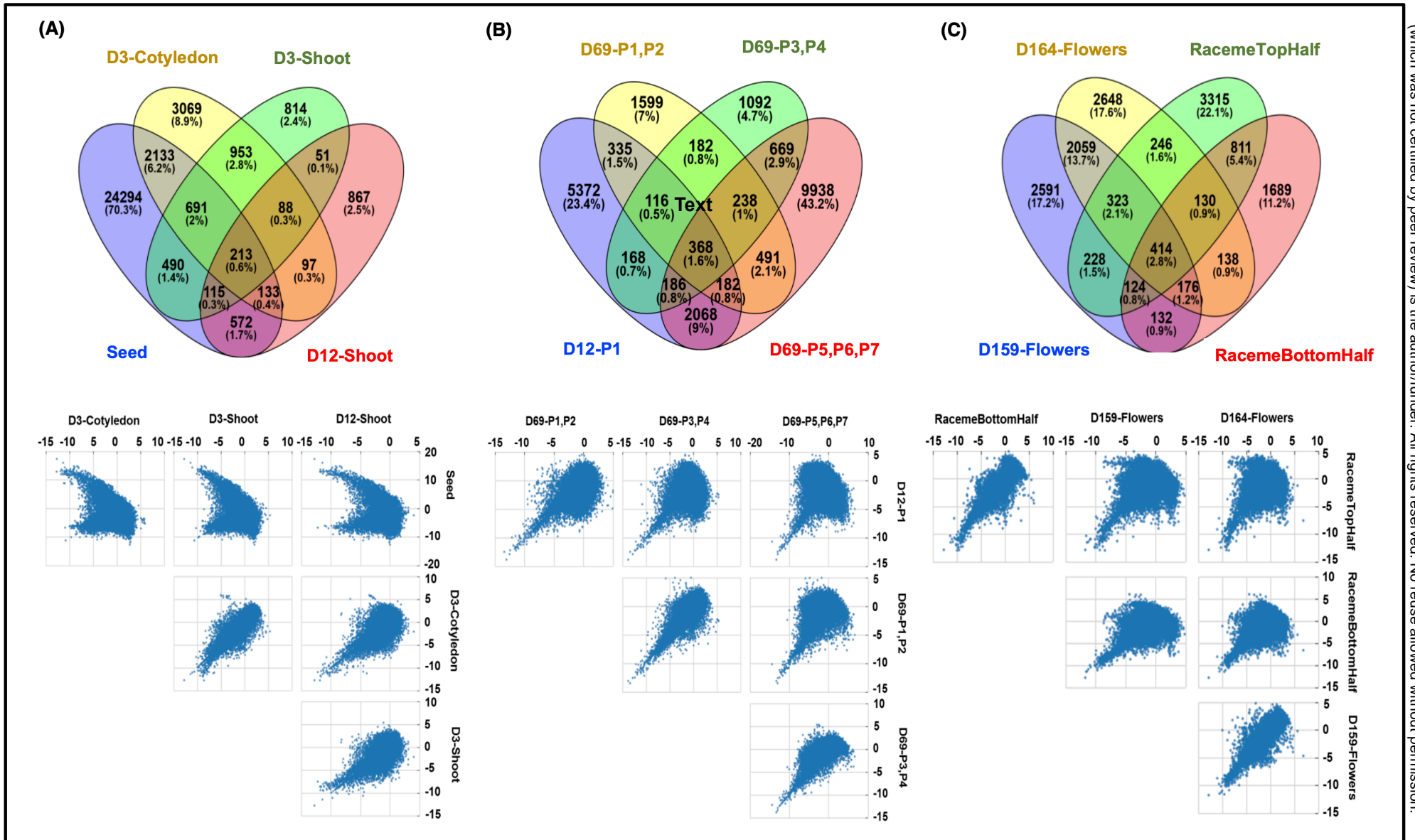


Figure 3



**Figure 4**

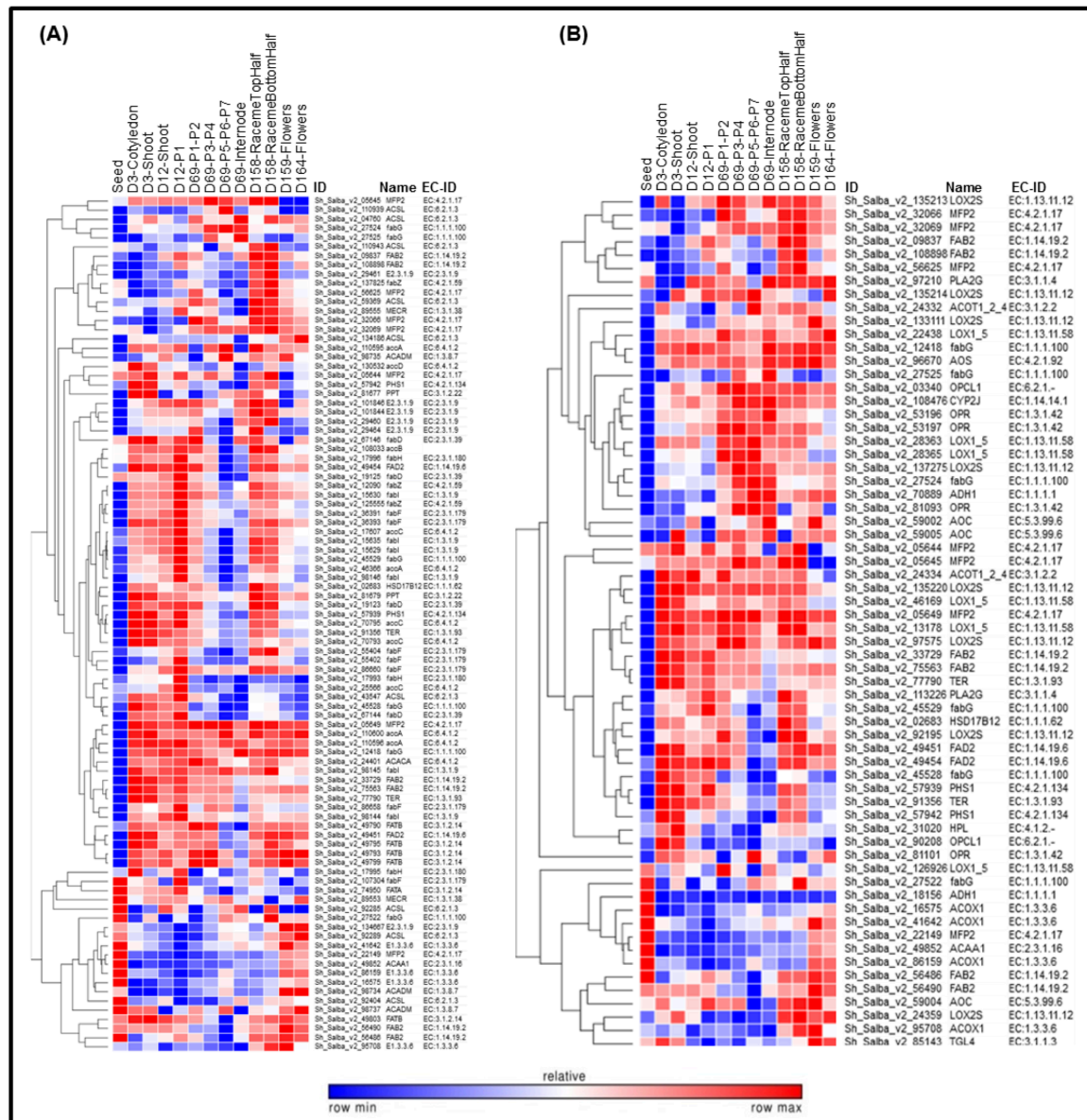




Figure 6

